Synvolcanic and Younger Plutonic Rocks from the Blake River Group: Implications for Regional Metallogenesis

STEPHEN J. PIERCEY,[†],[*]

Mineral Exploration Research Centre, Department of Earth Sciences, Laurentian University, Willet Green Miller Centre,
Ramsey Lake Road, Sudbury, Ontario, Canada P3E 2C6

ERIC C. CHALOUX,[**]

Resident Geologists Program, Ontario Geological Survey, Ministry of Northern Development and Mines,
Kirkland Lake, Ontario, Canada P2N 1A8

A. SHIRLEY PÉLOQUIN,[***]

Mineral Exploration Research Centre, Department of Earth Sciences, Laurentian University, Willet Green Miller Centre,
Ramsey Lake Road, Sudbury, Ontario, Canada P3E 2C6

MICHAEL A. HAMILTON,

Jack Satterly Geochronology Laboratory, Department of Geology,
University of Toronto, Earth Sciences Centre, 22 Russell Street, Toronto, Ontario, Canada M5S 3B1

AND ROBERT A. CREASER

Department of Earth and Atmospheric Sciences, University of Alberta, 126 Earth Sciences Building,
Edmonton, Alberta, Canada T6G 2E3

Abstract

The Blake River Group of the Abitibi greenstone belt is host to the well-known volcanogenic massive sulfide (VMS) deposits of the Noranda camp, Québec, Canada.

In the Noranda camp massive sulfide deposits are spatially associated with the coeval Flavrian-Powell intrusive complex, which is interpreted to have driven hydrothermal circulation that formed the deposits in the camp. In the western Blake River Group in Ontario there are also abundant intrusive rocks, yet relatively insignificant accumulations of VMS deposits. These intrusive rocks are younger (2686.9 ± 1.2 and 2688.5 ± 2.3 Ma) and are associated with porphyry-style Cu-Mo-Au mineralization with Re-Os molybdenite ages of 2682.4 ± 5 Ma. The intrusions are also smaller in areal extent and do not have a temporally extended, polyphase history like the Flavrian-Powell intrusive complex.

The intrusions of the western Blake River Group can also be distinguished by lithogeochemical attributes and a distinct petrological history compared to the Flavrian-Powell intrusive complex. They have lower total Y, Yb, Th, HFSE, and REE, with higher Zr/Y, La/Yb, Sm/Yb, Al_2O_3/Yb, and La/Sm$_{UCN}$ ratios, and lower Zr/Nb, Zr/Th, Zr/La, Zr/TiO$_2$, and Nb/Th$_{UCN}$ ratios. Petrologic modeling is consistent with the western Blake River Group intrusive rocks being generated as relatively low temperature melts (<800ºC) at depths >40 km in the crust where garnet is stable in the residue (e.g., garnet amphibolite residue). In contrast, modeling of the Flavrian-Powell intrusive complex is consistent with melting at shallower levels in the crust (e.g., <40 km) in the amphibolite stability field and at temperatures >800º to 850ºC. The occurrence of high-temperature magmatism at high levels within this crust that is coeval with volcanic activity explains the occurrence of numerous VMS deposits with the Flavrian-Powell intrusive complex, as this intrusive complex would have generated abundant heat at high levels in the crust to drive hydrothermal circulation. In contrast, the intrusions of the western Blake River Group were generated at depth and at lower temperature, increasing the probability of heat loss upon emplacement from depth, hence, decreasing the probability of hydrothermal circulation at high levels in the crust and likely explaining the paucity of VMS mineralization associated with these intrusive rocks. The petrological attributes of the Flavrian-Powell intrusive complex and western Blake River Group may be useful in delineating potentially fertile versus less prospective intrusive complexes in greenfields exploration areas.

Notably, the western Blake River Group intrusions have geochemical features similar to some Phanerozoic porphyry Cu-Mo-Au–associated intrusive systems consistent with the observed mineralization and highlighting the potential of porphyry Cu-Mo-Au systems of Late Archean age elsewhere in the Abitibi.

[†] Corresponding author: e-mail, steve_piercey@mac.com

[*] Present address: Stephen J. Piercey Geological Consulting, 11 First Avenue, St. John's, Newfoundland, Canada, A1B 1N3, and Department of Earth Sciences, Memorial University of Newfoundland, St. John's, Newfoundland, Canada, A1B 3X5.

[**] Present address: Copper Cliff North Mine, Inco Ltd., 18 Rink Street, Copper Cliff, Ontario, Canada P0M 1N0.

[***] Present address: First Nickel Inc., 2799-2 Belisle Drive, Val Caron, Ontario, Canada P3N 1B3.

Introduction

THE ARCHEAN Blake River Group of the Abitibi greenstone belt has been the focus of significant mining and mineral exploration for over a century and has contributed significant base metal and gold resources to the Canadian and international economy. The Noranda camp in Québec has produced over 3 million metric tons (Mt) of Cu and Zn from Cu-Zn (Noranda-type) volcanogenic massive sulfides (VMS) in 17 past-producing mines from within the Noranda cauldron (Gibson and Watkinson, 1990; Racicot, 1990). Significant gold also has been produced from the Au-rich Horne, Quemont, and Bouchard-Hébert mines (formerly Mobrun mine) in Noranda, Québec (Barrett et al., 1991; Kerr and Gibson, 1993; Riopel et al., 1995; Gibson et al., 2000) and the Bousquet and LaRonde mines in the Bousquet area, Québec (Dubé et al., 2007; Mercier-Langevin et al., 2007a-c). Including the Au-rich massive sulfide systems, the total past production and current reserves of VMS deposits in the Blake Rier Group exceeds 200 to 300 Mt (Galley et al., 2007).

The Flavrian-Powell intrusive complex forms the geologic roots to the Noranda VMS camp and is spatially associated with massive sulfide (Goldie, 1978, 1979). It has been interpreted to be the subvolcanic intrusive complex (or heat engine) that drove hydrothermal circulation in the Noranda camp (Galley, 2003). This spatial, and likely genetic, relationship between VMS mineralization and subvolcanic intrusive complexes is also present in many other VMS districts globally (Goldie, 1978; Campbell et al., 1981; Paradis et al., 1988; Galley, 1996, 2003; Brauhart et al., 1998; Piercey et al., 2003; see also Richards, 2003, and Richards and Kerrich, 2007; Whalen et al., 2004). In the western Blake River Group in Ontario, there are numerous intrusive complexes spatially associated with volcanic rocks, yet there are only minor VMS-style (e.g., Canagau) and breccia pipe-hosted Cu-Mo-Au

(e.g., Croxall) occurrences (Jensen, 1975; Hannington et al., 2003; Watkins and Melling, 2004; Chaloux, 2005). This raises the questions: what is unique about the Flavrian-Powell intrusive complex and why is it associated with so much mineralization (e.g., >100 Mt), whereas the intrusions of the western Blake River Group are relatively poorly endowed?

In this paper we compare the intrusive rocks of the western Blake River Group in Clifford Township with the Flavrian-Powell intrusive complex in the Noranda camp to better understand these relationships. The paper provides new field relationships derived from geologic mapping and logging of drill core, as well as lithogeochemical data and U-Pb zircon and Re-Os molybdenite geochronological data. We demonstrate that most of the intrusive rocks in the western Blake River Group are much younger than the Flavrian-Powell intrusive complex and associated volcanic rocks, were generated at lower temperatures and deeper in the crust than the Flavrian-Powell intrusive complex, have distinct lithogeochemical characteristics, and are spatially associated with porphyry-style Cu-Mo-Au mineralization. The petrological characteristics of the intrusive rocks of the western Blake River Group may help distinguish potentially prospective versus less prospective intrusive complexes in VMS environments, and the results have implications for similar VMS belts globally.

Regional Geologic and Tectonic Setting

The Blake River Group of the Abitibi subprovince of the Superior province (Card and Poulsen, 1998) consists of an approximately 10-km-thick sequence of basaltic through rhyolitic volcanic rocks (e.g., Dimroth et al., 1982; Gibson and Watkinson, 1990; Peloquin et al., 1990; Péloquin, 1999) that extends from Cadillac Township in Québec to Benoit Township in Ontario (Fig. 1). The Blake River Group in Ontario is located south of the Destor-Porcupine fault and lies north of
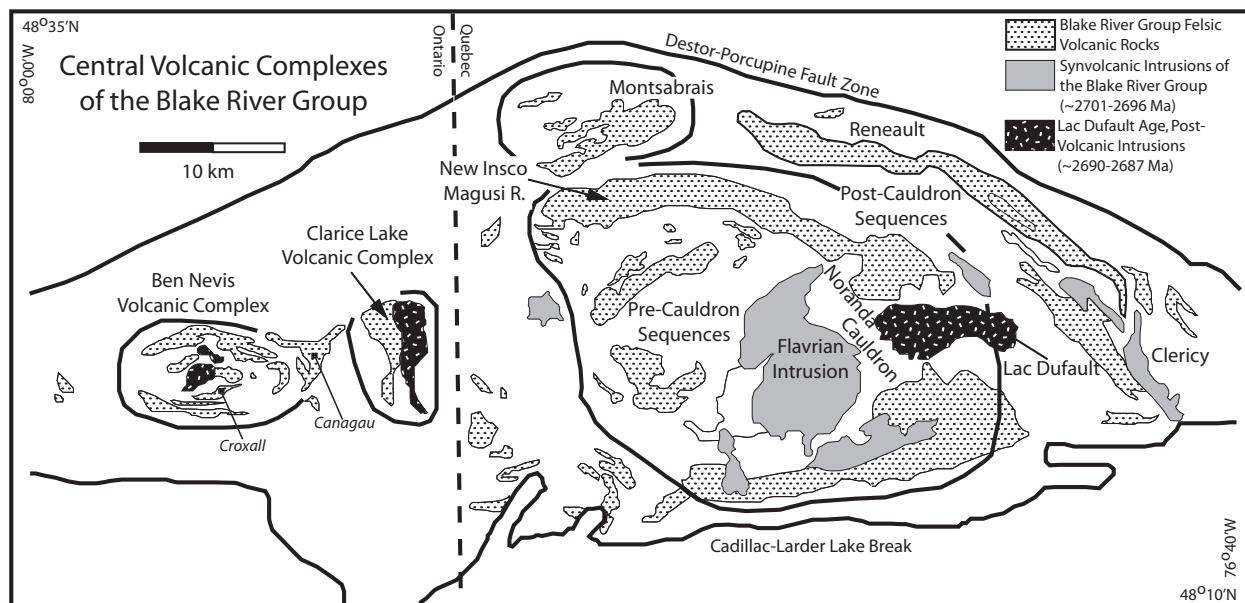

FIG. 1. Regional distribution of the Blake River Group (upper and lower bounds between the Destor-Porcupine fault and the Cadillac-Larder Lake break), with locations of major felsic volcanic complexes of the Central Blake River Group, synvolcanic intrusions of the Blake River Group, and younger Lac Dufault-age intrusions. Figure modified from Hannington et al. (2003).

the Cadillac-Larder Lake break primarily in Pontiac, Ossian, Ben Nevis, and Clifford Townships (Hogg, 1964; Jensen, 1975). It lies in unconformable contact with the underlying tholeiitic rocks of the Lower Blake River assemblage (formerly Kinojevis assemblage; e.g., Dimroth et al., 1982; Jensen, 1985; Jensen and Langford, 1985; Fowler and Jensen, 1989; Ayer et al., 2002), and in a regional sense, is overlain by rocks of the younger Porcupine and Timiskaming assemblages (Ayer et al., 2002). Uranium-lead zircon ages for volcanic rocks of the Blake River Group in both Québec and Ontario range from 2701 to 2694 Ma (Corfu et al., 1989, and references therein; Corfu, 1993; Mortensen, 1993; Galley and van Breemen, 2002). The Blake River Group is intruded by 2701 to 2696 Ma synvolcanic plutons (Goldie, 1978; Corfu and Noble, 1992; Galley and van Breemen, 2002; Galley, 2003) and numerous 2690 to 2689 Ma (Corfu, 1993; Mortensen, 1993; Chown et al., 2002) syn- to post-tectonic tonalite-trondjhemite-granodiorite (TTG) suite intrusions (Jensen, 1975; Feng and Kerrich, 1992; Sutcliffe et al., 1993; Péloquin and Piercey, 2003).

In Ben Nevis and Clifford Townships in Ontario (Fig. 2) the Blake River Group has been folded into dome-shaped patterns with stratigraphy facing outward from the Clifford stock (Jensen, 1975; Piercey et al., 2004). Here, the Blake River Group is cut by high-angle north-northwest– and east-northeast–trending strike-slip faults (Fig. 2). The metamorphic grade is greenschist to subgreenschist facies in Québec, whereas in Ontario the rocks are at prehnite-pumpellyite facies (Jolly, 1980; Powell et al., 1993, 1995; Hannington et al., 2003). Locally, in contact aureoles around intrusions the Blake River Group rocks are metamorphosed to albite-epidote-magnetite facies (Jensen, 1975; Piercey et al., 2004).

Field, geologic, and geochemical attributes have led to various interpretations for the tectonic setting of the Blake River Group. In recent years, most workers have suggested that the Blake River Group represents an arc to back-arc basinal geodynamic setting (Lafleche et al., 1992a, b; Ludden and Peloquin, 1996; Péloquin, 1999; Wyman et al., 2002; Wyman, 2003), with potential for plume-arc interaction (Wyman, 2003; Wyman et al., 2002). The later ~2.69 Ga TTG suite magmatism that postdates the Blake River Group is interpreted to reflect TTG generation via slab melting, potentially due to melting of mafic to ultramafic slab material due to flat subduction (Wyman et al., 2002; Wyman, 2003). Alternatively, autochthonous models for the Blake River Group may also be applicable (Ayer et al., 2002; see also Bedard, 2006)

Previous Work

The Blake River Group in Clifford Township has been the focus for a number of years. The most detailed regional mapping in Clifford Township was undertaken by Jensen (1975), which updated the previous work of Wilson (1901), Knight (1920), and Gledhill (1928). The Jensen and Langford (1985) study provided a regional stratigraphic framework, which is the basis for most of the mapping and stratigraphic work in this paper.

Wolfe (1977) conducted a volcanic lithogeochemical and soil and till geochemical study of Ben Nevis Township and showed anomalous Zn and Cu values in volcanic rocks with larger areas enriched in As, Sb, Pb, Li, Sn, and Hg. Grunsky

(1986) undertook a regional alteration lithogeochemical study of the volcanic rocks in Clifford and Ben Nevis Townships and outlined various types and zones of alteration and mineralization. This work was refined by Grunsky and Agterberg (1988) and Grunksy (1988). In the 1990s, regional-scale hydrothermal alteration was examined by Galley (2003) and Hannington et al. (2003).

Recently, fluid inclusion studies of quartz- and epidote-associated mineralization were undertaken by Ioannou et al. (2004) and Weiershäuser and Spooner (2005). Their work illustrated that most of the quartz associated with mineralization was of low-temperature (110º–160ºC) hydrothermal origin with relatively low to moderate salinities, likely due to semiconformable alteration in a VMS environment. This study also summarizes recent regional thematic mapping of key areas of the volcanic stratigraphy of Ben Nevis Township and detailed studies of the Clifford stock and related mineralization in Clifford Township (Chaloux, 2005; MacDonald et al., 2005; this study).

Geology and Stratigraphic Relationships

The geologic and stratigraphic relationships of the Blake River Group and Clifford stock in Clifford Township were established by bedrock geologic mapping and examination of drill core (Figs. 2, 3). Clifford Township is dominated by volcanic and subvolcanic rocks of the Blake River Group, felsic intrusive rocks of the Clifford stock and associated dikes (referred to hereafter as the Clifford intrusive complex), and Paleoproterozoic diabase of the Matachewan dike swarm (Figs. 2, 3). The volcanic rocks consist of basaltic-andesite, andesite, and felsic volcaniclastic rocks that young outward from the Clifford stock (Fig. 2). The stratigraphy is interpreted to record two cycles of volcanism and comprises five volcanic to volcaniclastic units as well as synvolcanic diabase and/or gabbro intrusions. The lowermost packages consist of pillowed to massive basaltic andesite to andesite that is amygdaloidal and variably plagioclase porphyritic; plagioclase phenocrysts are 2 to 3 mm long and euhedral. Conformably overlying the amygdaloidal basaltic andesite is an andesitic volcaniclastic unit. The andesitic volcaniclastic rocks are matrix supported and consist of fine-grained, gray to gray-black andesitic tuff with varying amounts of feldspar lapilli and black andesitic fragments. Feldspar grains range from <1 to 5mm and are euhedral to subhedral; in places they comprise 30 to 40 vol percent of the rock. Black andesitic fragments are subrounded to subangular, range from <1 up to 10 cm in size, and constitute up to 20 to 30 vol percent of the rock. Overlying the andesitic tuff unit is the first of two felsic volcaniclastic units consisting of a matrix-supported felsic tuff breccia (nomenclature from Fisher, 1966). On surface these tuff breccias appear monolithic to polylithic. However, in drill core the breccias are polylithic with clasts of andesite, basaltic-andesite, dacite, and rhyolite; all clasts are angular to subrounded, occur within a matrix of fine siliceous ash, and range in size from 1 to 30 cm.

Overlying the first felsic volcaniclastic unit is a second unit of amygdaloidal and variably plagioclase porphyritic basaltic-andesite to andesitic tuff with small plagioclase feldspars less than 1 and up to 2 to 3 mm. The uppermost stratigraphic unit consists of a second felsic tuff breccia to lapilli tuff, very

FIG. 2. Geologic map of the Clifford stock and the Blake River Group, Clifford Township, Ontario. Geology based on the mapping of Piercey et al. (2004), Péloquin and Piercey (2005), and Jensen (1975). Line A-B is the line of stratigraphic column in Figure 3.
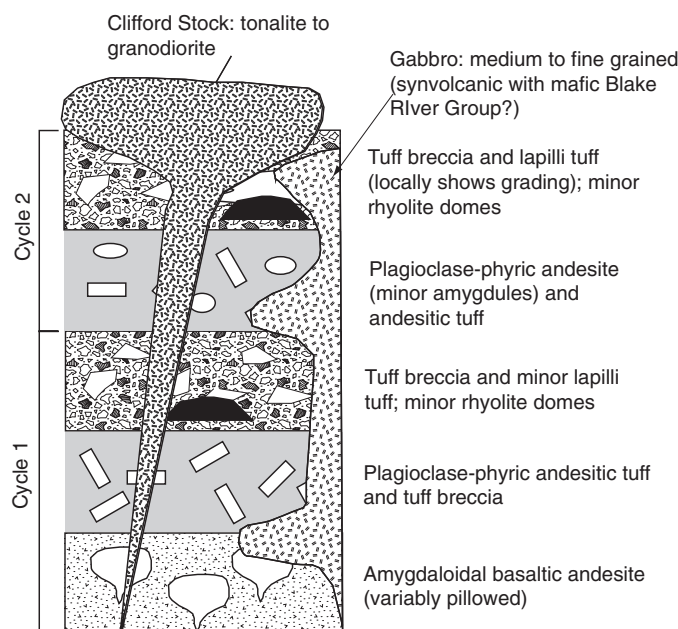
FIG. 3. Schematic stratigraphic column for rocks of the Blake River Group in Clifford Township (from Piercey et al., 2004).

similar to the underlying tuff breccia, consisting of a matrix-supported breccia with angular clasts of dacite to rhyolite. Normal grading in the tuffs and tuff breccia and the transition from tuff breccia to lapilli tuff on a regional-scale are consistent with stratigraphic facing outward from the Clifford stock (Jensen, 1975).

Minor felsic flows and cryptodomes occur within Clifford Township. In southern Clifford Township felsic flows are associated with a primarily felsic volcaniclastic package (Fig. 2). These flows are white, aphyric, massive, and rhyolitic. In eastern Clifford Township there are flow-banded rhyolitic volcaniclastic rocks (Fig. 4A) spatially associated with synvolcanic rhyolitic dikes (Fig. 4B), interpreted to be part of a cryptodome. The rhyolitic volcaniclastic rocks in eastern Clifford Township are different from most felsic volcaniclastic rocks in the area in that they are clast-supported, mono-lithologic, and consist of polygonally-jointed, flow-banded rhyolite fragments (Fig. 4A). Rhyolitic intrusive rocks that intrude these felsic volcaniclastic rocks have irregular margins, are fine grained, and are synvolcanic (Fig. 4B; see Péloquin et al., 2008, for U-Pb geochronology of these dikes).

Mafic intrusive units cutting the Blake River Group stratigraphy are often difficult to distinguish from the mafic-intermediate volcanic rocks of the Blake River Group. These rocks intrude all stratigraphic units of the Blake River Group but have chemical attributes similar to those of the volcanic rocks (see MacDonald et al., 2005) and are synvolcanic to the basaltic-andesitic to andesitic volcanic rocks. The intrusions form sheet-like and dike-like intrusions of diabase, diorite, and locally gabbro. In some places the dike-like intrusions have amygdules suggesting emplacement at high levels, also supporting a synvolcanic origin (e.g., Jensen, 1975).

The Blake River Group is intruded by granitoids of the Clifford Stock and by east-northeast-trending dikes interpreted to be equivalents of the Clifford Stock (Figs. 2, 3). The

Clifford Stock itself consists of a relatively equigranular tonalite to granodiorite, commonly hornblende-bearing and locally hornblende-biotite-bearing (Fig. 4C-D). Xenoliths of the surrounding wall rock are present in the intrusion locally. Southeast of the Clifford stock are numerous east- to northeast-striking dike- to sill-like intrusions that cut the Blake River Group (Figs. 2, 3). These dikes are fine- to medium-grained, variably feldspar porphyritic, locally pyrite-bearing, siliceous, and dacitic to rhyolitic in composition (Fig. 4E). The felsic dikes have straight walls in most places, suggesting emplacement into solidified host rock material, but are irregular in some localities as a result of emplacement into dilatent zones or when associated with hydrothermal brecciation. The dikes contain xenoliths of very angular fragments of wall rock and the breccias are interpreted to be due to forceful emplacement of the dikes into their hosts (Fig. 4F). They are also spatially associated with breccia pipes (e.g., Croxall occurrence) and stockworks of pyrite-quartz-gold-molybdenite veins (Chaloux, 2005).

The granitoids are cut by north-northwest–trending dikes of the 2.47 to 2.45 Ga Matachewan mafic dike swarm (Fig. 2; Heaman, 1997). These gabbroic dikes are coarse grained, have no recrystallization of primary igneous mineralogy, and are highly magnetic, unlike the synvolcanic gabbro-diabase intrusions of the Blake River Group.

Alteration and Mineralization Styles

Alteration and mineralization within Clifford Township includes (1) contact metamorphic alteration around the Clifford stock with minor pyrite mineralization, (2) synvolcanic VMS-style alteration and mineralization, and (3) intrusion-related or porphyry-style alteration and subeconomic Cu-Mo-Au mineralization.

Regional metamorphic assemblages are dominated by low-grade prehnite-pumpellyite facies minerals (Jensen, 1975; Hannington et al., 2003). Near the Clifford stock a well-defined contact metamorphic aureole surrounds the intrusion for 200 to 300 m (Fig. 2). In the aureole, the basaltic-andesitic to andesitic rocks exhibit a distinctive greenish-black coloration and contain magnetite, lathlike needles of plagioclase (albite), epidote patches, and, in some cases, a fibrous to needlelike amphibole (actinolite; Fig. 5A). Minor disseminated pyrite is present in the metamorphic aureole.

Synvolcanic VMS-style alteration is characterized by amygdule-filling chlorite, quartz, epidote, and/or pyrite (Fig. 5B). Most common are quartz-pyrite fillings but there are also epidote-quartz-pyrite, chlorite-quartz, and chlorite-pyrite infillings. These mineral assemblages are also present in the more mafic members of the Blake River Group, as patches, typically near permeable zones in the rocks (i.e., in hyaloclastite or volcanic breccias). These alteration assemblages are interpreted to represent semiconformable alteration (cf. Galley, 1993). Silicification and chlorite alteration are associated with sulfide mineralization and interpreted to be vent proximal, high-temperature alteration (e.g., Franklin et al., 2005; Galley et al., 2007). This style of alteration and mineralization has been observed only in drill core within the lowermost basaltic-andesite pillow lava sequence. Associated mineralization is restricted to hyaloclastite along pillow margins where chalcopyrite, pyrite, and quartz are found interstitial to angular
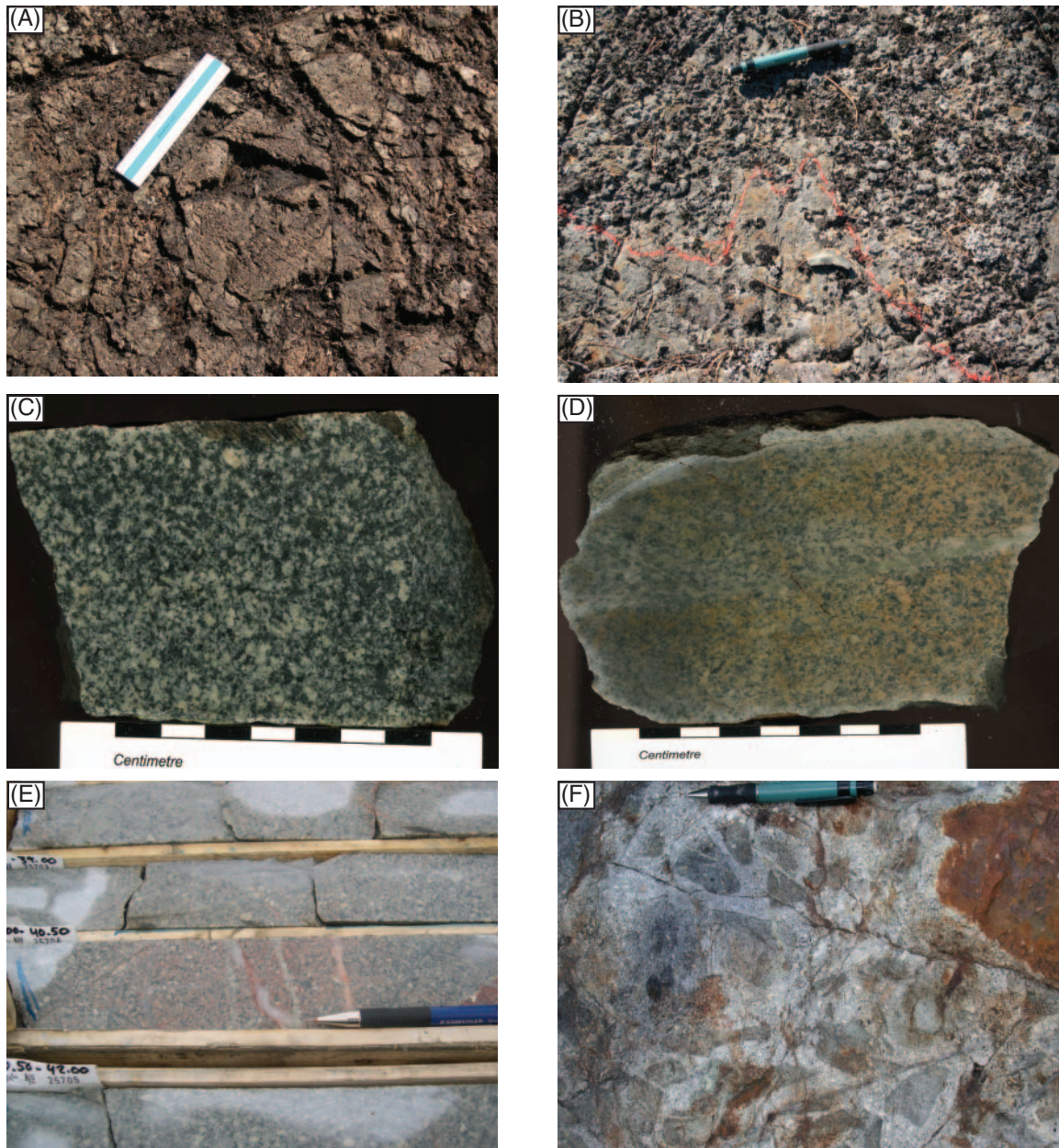
FIG. 4. A. Monolithologic carapace breccia of rhyolite with polygonally jointed, flow-banded rhyolite clasts from the western part of Ben Nevis Township. B. Synvolcanic rhyolite dike (bottom of photo) with irregular margins intruding into flow-banded rhyolite carapace breccia. C. Typical hornblende tonalite from the Clifford stock. D. Finer grained border phase from the western margin of the Clifford stock. E. Finer grained porphyry dikes that are equivalent to the Clifford stock (note crosscutting veins). F. Typical dike with brecciated xenoliths of surrounding wall rock, suggesting a forceful emplacement.

FIG. 5. Photographs of mineralization and alteration types from Clifford Township. A. Recrystallized basaltic andesite of the Blake River Group with albite (white laths) and magnetite (black clots) from the contact aureole of the Clifford stock. B. Amygdaloidal andesite from the Blake River Group with amygdules filled with epidote, chlorite, and pyrite; this assemblage is typical of VMS-related regional semiconformable alteration (e.g., Galley, 1993). C. Pillow lava with chlorite alteration of the edge of the pillow with silicification of the hyaloclastite (white fragments), and pyrite-chalcopyrite mineralization; this is typical of pipelike VMS-related alteration. D. Breccia pipe occurrence from the Croxall prospect with angular andesite fragments in a matrix of quartz and sulfide; this style of alteration is interpreted to represent a younger magmatic-hydrothermal event. E. Pyrite-rich assemblage associated with the breccia pipe at the Croxall prospect. F. Randomly oriented epidote-quartz veins that are associated with the younger, magmatic-hydrothermal event (i.e., these veins cut the Clifford stock as well, thus must be post ~2690 Ma). G. Medium to dark gray quartz veins that contain pyrite, molybdenite, and gold; these veins typically form stockworks and are interpreted to reflect a magmatic (porphyry)-style of mineralization (Chaloux, 2005). H. Typical late "J-veins" (jasper veins) of K-feldspar, calcite, and hematite; these veins are the latest in the magmatic-hydrothermal paragenesis and crosscut all other alteration and mineralization.
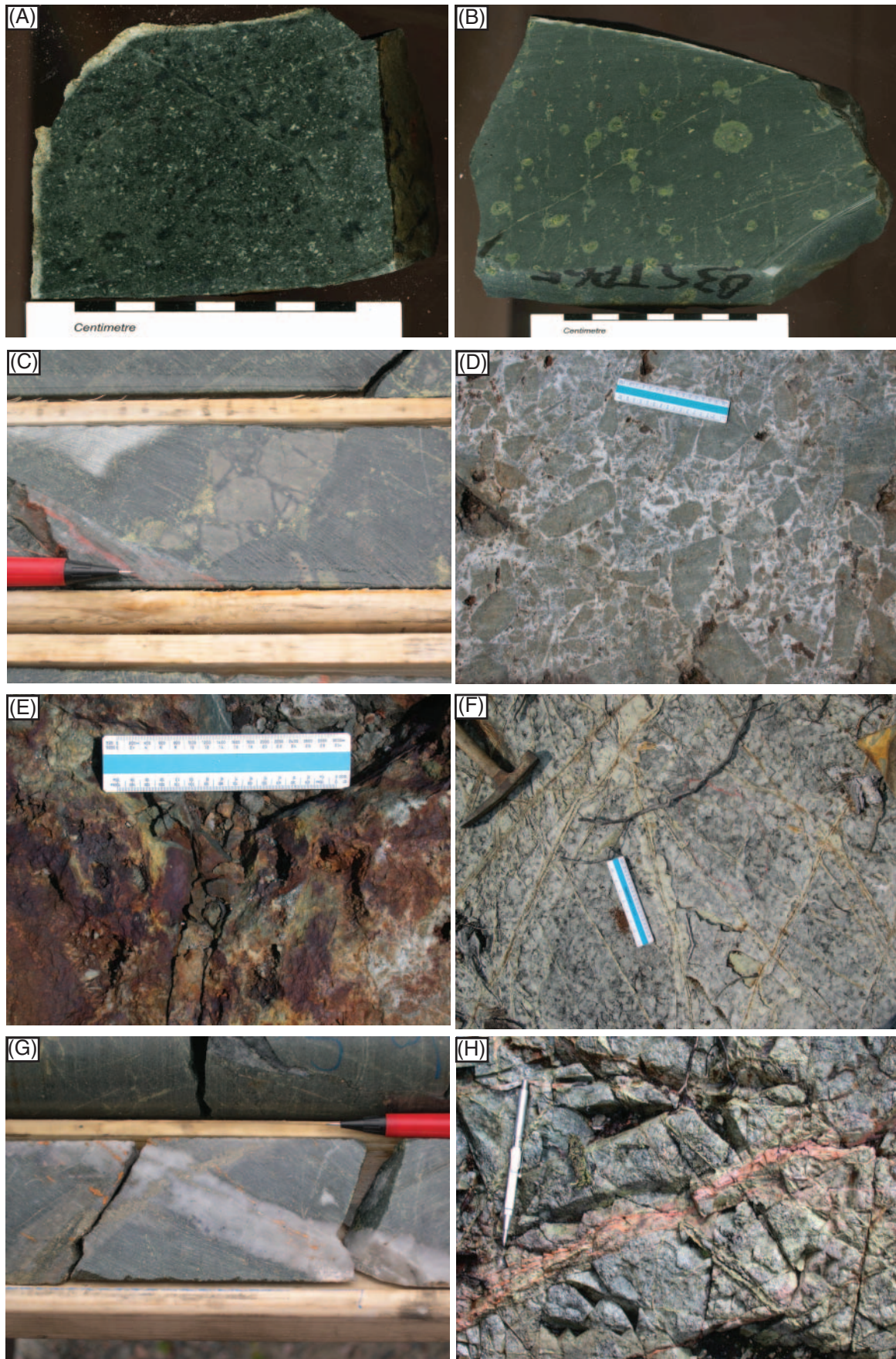
hyaloclastite with sulfides comprising a maximum of ~10 vol percent of the rock (Fig. 5C). Hyaloclastite fragments are either bleached to a white-pink color and silicified or are completely altered to chlorite ± epidote (Fig. 5C). Finer grained ash-sized material in the matrix of the hyaloclastite is commonly completely replaced by chlorite.

Porphyry Cu-Au-Mo–style alteration is associated with breccia pipe occurrences on surface (e.g., Croxall; Figs. 2, 6) and with felsic dikes and breccias in drill core (Fig. 5) and overprints VMS-style alteration. On surface the mineralization occurs within breccia pipes, like the Croxall prospect (Fig. 6). These pipes are circular in nature, dominated by porphyry and brecciated rhyolite porphyry, and are hosted by andesitic rocks. At the Croxall prospect there is a zoned breccia pipe with a core of andesitic breccia (collapse breccia) with interstitial quartz and sulfide cement (Fig. 5D), which grades out to a "milled" marginal breccia enriched in quartz, pyrite, and chalcopyrite (Figs. 5E, 6) with elevated Au, Ag, and Mo (Chaloux, 2005). Silicification and pyrite alteration occurs in the breccia pipe, whereas outside of the breccia pipe wall rocks have a randomly oriented network of millimeter- to centimeter-scale veins consisting of quartz, epidote, K-feldspar, hematite, and calcite (±sericite; Fig. 5F-H). In drill core, mineralization and alteration are associated with a randomly oriented vein network that exhibits a complex paragenesis. The paragenesis appears to be, from oldest to youngest, (1) epidote, chlorite, and sericite (Fig. 5F), (2) quartz-pyrite, (3) dark gray quartz-pyrite-chalcopyrite-molybdenum (and gold?, Fig. 5G), and (4) hematite-calcite- ±K-feldspar (Fig. 5H). Cu-Mo-Au mineralization is associated with dark gray quartz veins, and the aleration is cut by late hematite-calcite ±K-feldspar veins, similar to "J veins" in porphyry systems (due to their jasperoidal appearance). The veins that host

mineralization are present in all rock types but most of the mineralization occurs in feldspar porphyritic rhyolite dikes with compositions similar to the Clifford stock. These relationships provide compelling evidence that the porphyry-style mineralization is a younger hydrothermal event that postdates, but is likely related to, the emplacement of the Clifford stock and associated dikes (see U-Pb and Re-Os geochronology below).

Lithogeochemistry

The lithogeochemical data for the Clifford stock and associated dikes are presented in Table 1. Geochemical samples were collected from surface exposures and weighed ~1 kg. Weathered surfaces were removed in the field or with a diamond saw. Samples were crushed using a steel jaw crusher and subsequently pulverized. Samples from 2003 were pulverized in an agate mortar at the Ontario Geoscience Laboratories in Sudbury, Ontario, and samples from 2004 were pulverized in mild steel at Activation Laboratories in Ancaster, Ontario. Samples pulverized in the mild steel mortar may have up to 0.2 percent contamination by Fe, with contamination from other trace elements being negligible (E. Hoffman, pers. commun., 2007). Samples crushed in agate can have minor Si contamination. Powders were analyzed using a combination of X-ray fluorescence (XRF), inductively coupled plasma emission spectroscopy (ICP-ES), and inductively coupled plasma mass spectrometry (ICP-MS). Major elements were determined by wavelength dispersive XRF using fused disks at both the Ontario Geoscience Laboratories (2003 samples) and Activation Laboratories (2004 samples); LOI was determined via conventional heating and weight difference methods at both the laboratories. Trace elements were analyzed via inductively coupled plasma mass spectrometry (ICP-MS: Nb, Ta, Zr, Hf, Y, Cs, Th, U, La, Ce, Pr, Nd, Sm, Eu, Gd, Tb, Dy, Ho, Er, Tm, Yb, Lu) and inductively coupled plasma emission spectroscopy (ICP-ES: Ba, Be, Cd, Co, Cr, Cu, Li, Mo, Ni, S, Sc, Sr, V, W, Zn), using a closed-beaker multiacid digestion method prior to analysis (Burnham et al., 2002; Burnham and Schweyer, 2004) at the Ontario Geoscience Laboratories. Some trace elements were also determined by pressed powder pellet XRF at the Ontario Geoscience Laboratories (2003 samples: Nb, Zr, and Y) and Activation Laboratories (2004 samples: Nb, Zr, Y, Ni, Cr, and V). Niobium, Zr, and Y were all determined by XRF pressed pellet analysis to test whether digestions were complete for ICP-ES and ICP-MS methods. Most samples the XRF Nb, Zr, and Y were within 10 percent of the values obtained by ICP-MS, suggesting that the dissolutions were complete. Niobium, Zr, and Y data by ICP-MS are utilized in this paper because of the superior detection limits and sensitivity for these elements by ICP-MS as compared to XRF. The 2003 samples have Ni, Cr, and V values via ICP-ES from the Ontario Geoscience Laboratories, whereas the 2004 samples have utilized Ni, Cr, and V via pressed pellet XRF from Activation Laboratories. For most samples, the Ni, Cr, and V values via XRF are within 10 percent of the samples analyzed by ICP-ES. Precision was determined using duplicate analyses and reference materials (see details in MacDonald et al., 2005). Precision for major elements by XRF was 2 to 5 percent (except MgO = 7% and P2O5 = 10%). Precision for trace
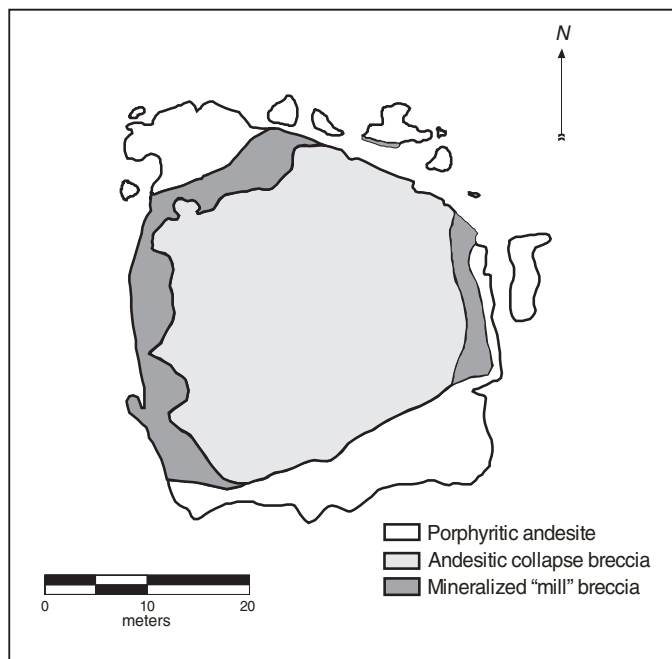

FIG. 6. Geologic map of the Croxall breccia pipe, illustrating the rounded, pipelike nature of the pipe with mineralization located on the margins of the pipe (from Chaloux, 2005).

elements by ICP-ES analysis at the Ontario Geoscience Laboratories are Ba (5%), Be (5%), Co (15%), Cr (15%), Cu (15%), Li (10%), , Ni (10%), S (20%), Sc (10%), Sr (10%), V (10%), and Zn (10%). Precisions for trace elements by ICP-MS are Nb (5%), Ta (5%), Zr (10%), Hf (10%), Y (10%), Cs (10%), Th (7%), U (7%), and REE (<10–12%). Estimated accuracy, based on analysis of reference materials, can be found in MacDonald et al. (2005).

Results

Geochemical data for the Clifford intrusive suite rocks are presented in figures that follow and Table 1. The rocks of the Clifford intrusive suite have SiO_2 contents of 60 to 70 wt percent and, for the most part, have Na_2O contents of 2 to 5 wt percent and Al_2O_3/Na_2O values <10 (Fig. 7). Most samples have LOI values <4 wt percent and there is an antipathetic relationship between Na_2O and LOI (Table 1), suggesting that the lower Na_2O contents are due to Na losses associated with weak alteration. Major element compositions tend to deviate little from primary igneous compositions (Fig. 7B-C), however, suggesting that most rocks are only weakly altered. The normative mineralogy for the Clifford intrusive suite suggests that the rocks are primarily tonalite, trondjhemite, and granodiorite (TTG; Fig. 8A). The Clifford intrusive suite has calc-alkaline affinities on an AFM plot (Fig. 8B) and generally subalkaline Nb/Y ratios (Winchester and Floyd, 1977; modified by Pearce, 1996; Fig. 8C). The suite has relatively high Al_2O_3 contents (>13%) and low Yb (≤ 2 ppm), consistent with them being part of a high Al TTG suite (Fig. 8D). The low Yb concentrations in samples of the Clifford intrusive suite are matched by very low Y concentrations (typically less than 10 ppm; Table 1) and they have very high, calc-alkaline Zr/Y ratios (>7) characteristic of the FI rhyolites of Lesher et al. (1986; Fig. 9A).

The primitive mantle-normalized patterns for the Clifford intrusive suite are light rare earth element (LREE) enriched with heavy rare earth element (HREE) depletions, negative Nb, Ti, and Eu anomalies, positive Zr, Hf, and Al anomalies, and depletions in compatible elements (Fig. 9B). The low contents of the HREE (i.e., Yb) and Y and Sc/Y ratios ~0.5 to 1.0 (Fig. 9C) are consistent with garnet and hornblende (e.g., Feng and Kerrich, 1992) residing in the source from which the Clifford intrusive suite were partially melted (i.e., generation at high pressures; see below).

U-Pb Geochronology

To constrain the age of the Clifford stock and associated dikes two samples were collected for U-Pb zircon geochronology, including a sample from the Clifford stock and a dike interpreted to be related to it. Both samples were analyzed at the Jack Satterly Geochronology Laboratory at the University of Toronto. Weathered surfaces were removed in the field, and each piece was subsequently washed and dried in the laboratory before further processing following the methods of Ayer et al. (2005) and Thurston et al. (2008). Zircons were obtained from 10- to 15-kg samples using standard methods involving crushing, grinding, Wilfley table, heavy liquid, and magnetic separation methods. The highest quality zircons were handpicked from the least paramagnetic groups with the highest quality zircon grains selected on the

basis of clarity, and the absence of cores, cracks, alteration, and (Pb-bearing) inclusions. All zircon fractions were subjected to an air abrasion treatment (Krogh, 1982) and then subsequently dissolved and spiked following the methods of Ayer et al. (2005) and Thurston et al. (2008). Isotopic compositions of Pb and U were determined on a VG354 mass spectrometer at the Jack Satterly Geochronology Laboratory where procedural blanks are routinely at the 0.5- and 0.1-pg level or less for Pb and U, respectively. Initial compositions of common Pb were estimated here after Stacey and Kramers (1975) and decay constants used are those recommended by Steiger and Jäger (1977). Age errors in the text and tables are all presented at the 95 percent confidence level. Error ellipses in the concordia diagrams are shown at the 2σ level. For concordant and near-concordant data having overlapping $^{207}Pb/^{206}Pb$ errors, weighted mean ages were calculated by forcing a regression through the origin of concordia, according to the method of Davis (1982). Uranium-lead concordia diagrams were generated using the IsoPlot/Ex program of Ludwig (2001). Calculated ages and errors using either the Davis (1982) or IsoPlot/Ex (Ludwig, 2001) algorithms were equivalent.

Age of Clifford stock

Sample 03SJP-115 (591133E, 5351000N, NAD83 datum) was collected to determine the primary crystallization age of the Clifford stock and to compare its age with other rocks of the Blake River Group, including subvolcanic intrusive rocks coeval with the Blake River Group stratigraphy. This sample is tonalitic to granodioritic in composition and is equigranular to weakly porphyritic with some larger 0.5-cm K-feldspar phenocrysts and/or megacrysts. Hornblende is the dominant mafic phase and there are some rounded epidote patches within the sample. Zircon within this sample is abundant and dominated by a population of elongate (length:width up to 6:1) cylindrical euhedral grains as well as subordinate, flat grains and larger, "glassy" fragments. Results from three analyzed single-grain fractions all overlap, straddling concordia, and a weighted mean $^{207}Pb/^{206}Pb$ age for all three is 2686.9 ± 1.2 Ma (±6.9 Ma including decay constant uncertainty; Fig. 10; Table 2). This age is younger than most ages in the Blake River Group that range from 2700.9 to 2694.1 Ma (Corfu et al., 1989; Mortensen, 1993; Galley and van Breemen, 2002).

The 2686.9 Ma age is interpreted to represent the timing of magmatic crystallization of the Clifford stock and is similar to that determined for the Clarice Lake pluton (Corfu and Noble, 1992), which also intrudes the Blake River Group near the Ontario-Québec border (Table 3). Emplacement of the Clifford stock also coincided in time with intrusion of the Lac Dufault pluton in the eastern Abitibi of Québec (Table 3), a late, K-feldspar porphyritic phase of the Lac Abitibi batholith (Mortensen, 1993, and references therein), the K-feldspar porphyritic Adams stock south of Timmins (Frarey and Krogh, 1986), and several gold-related intrusive rocks in the Porcupine camp (Corfu et al., 1989).

Age of felsic dikes

Sample 03SJP-059-1 (590369E, 5349181N, NAD83 datum) was collected from a representative felsic dike intruding andesitic volcaniclastic rocks. These dikes have straight margins

TABLE 1. Geochemical Data for Rocks of the Clifford Stock and Associated Dikes

Sample	03SJP013-2-1	03SJP013-2-1(2)	03SJP020-2	03SJP022-1	03SJP047-2-1	03SJP059-2	03SJP096-2-1	P03-007A	P03-007B
Easting	590880	590880	589170	589444	590849	590369	591934	590938	590938
Northing	5349453	5349453	5350097	5350567	5351742	5349181	5351663	5360770	5360770
Drill hole	-	-	-	-	-	-	-	-	-
Depth	-	-	-	-	-	-	-	-	-
Rock type	Diorite porphyry	Diorite porphyry	Tonalite/ granodiorite	Tonalite/ granodiorite	Tonalite/ granodiorite	Diorite porphyry	Diorite	Diorite	Diorite
SiO_2 (wt %)	70.18	61.95	62.86	60.59	60.82	62.91	58.63	60.36	61.27
TiO_2	0.57	0.62	0.59	0.64	0.59	0.44	0.68	0.62	0.63
Al_2O_3	13.63	16.84	16.64	17.98	17.53	16.29	17.53	17.66	17.95
Fe_2O_3	3.47	5.17	5.01	5.4	5.03	3.38	5.93	5.28	5.07
MnO	0.02	0.07	0.06	0.09	0.07	0.09	0.07	0.07	0.07
MgO	2.3	3.11	2.42	3.15	2.83	1.61	3.03	2.84	2.86
CaO	2.61	4.9	3.95	5.95	5.45	3.93	6.82	6.97	6.04
Na_2O	3.92	3.98	4.93	3.74	4.27	3.44	4.67	4.39	4.25
K_2O	1.16	1.07	1.12	1.01	1.42	2.97	1.11	0.92	1.05
P_2O_5	0.07	0.15	0.12	0.14	0.14	0.11	0.16	0.15	0.14
LOI	2.35	2.22	2.23	2.18	2.27	4.61	2.34	1.65	1.93
Total	100.28	100.1	99.92	100.87	100.43	99.79	100.98	100.9	101.26
Ni (ppm)	31	42	32	41	38	24	172	36	38
Cr	21	31.08	28.17	34.45	27.58	19.34	36.17	29.36	31.21
Co	20	17	16	20	17	12	22	17	16
V	69.6	86	76.5	94	81.7	54.4	154.2	87.6	91.5
Sc	8.1	7.2	5.5	7.9	6.9	4.3	8.8	7.5	7.9
Cu	281	153	19	102	115	229	2199	13	5
Zn	50	67	54	100	69	244	117	37	42
Cd	ND	ND	ND	ND	ND	ND	ND	ND	ND
Mo	ND	ND	ND	ND	ND	ND	ND	ND	ND
W	8	4	5	10	7	12	N.D.	N.D.	4
Nb (XRF)	7	7	6	7	7	4	8	5	5
Y (XRF)	19	12	13	8	9	8	29	8	8
Zr (XRF)	160	112	90	90	95	95	158	89	93
Zr	163.8	114.1	94.1	97.5	89.1	105	125.8	78.5	88.4
Hf	4.5	3.2	2.7	2.8	2.7	3	3.3	2.3	2.4
Nb	6.8	5.7	5.3	5.7	6.1	3.5	6.9	5.9	5.2
Ta	0.63	0.47	0.47	0.48	0.54	0.34	0.5	0.46	0.41
Y	18.03	10.5	12.96	8.65	8.97	8.58	8.82	8.69	8.26
Be	0.65	0.54	0.38	0.5	0.53	0.61	0.52	0.52	0.52
Li	11	16	10	12	17	8	20	16	24
Cs	0.966	1.072	0.934	1.247	1.54	1.933	0.835	0.717	0.758
Rb	46.29	33.47	45.17	27.44	49.58	83.16	38.95	24.53	31.33
Ba	166	311	242	296	332	422	247	231	248
Sr	143.5	271.6	232.3	299.7	240.4	195.9	266	341.4	324.5
Th	3.58	1.92	2.31	1.84	2.51	1.6	1.58	1.55	1.27
U	0.888	0.408	0.648	0.467	0.526	0.511	0.452	0.359	0.362
La	16.24	11.53	10.17	11.57	10.7	11.54	10.17	11.5	10.75
Ce	33.79	25.1	24.01	25.27	23.7	22.22	24.5	24.12	22.94
Pr	3.913	3.102	3.103	3.145	3.107	2.955	3.151	3.023	2.854
Nd	15.22	12.24	12.94	12.58	12.84	12.27	12.89	12.07	11.58
Sm	3.3	2.63	2.88	2.6	2.6	2.42	2.67	2.44	2.39
Eu	0.875	0.74	0.781	0.78	0.818	0.81	1.588	0.787	0.751
Gd	3.177	2.357	2.686	2.267	2.325	2.1	2.344	2.172	2.144
Tb	0.529	0.337	0.419	0.317	0.326	0.294	0.325	0.306	0.297
Dy	3.191	2.041	2.457	1.769	1.742	1.615	1.765	1.707	1.606
Ho	0.678	0.397	0.494	0.335	0.337	0.312	0.336	0.323	0.304
Er	2.034	1.129	1.449	0.918	0.913	0.862	0.892	0.867	0.829
Tm	0.309	0.166	0.212	0.132	0.128	0.125	0.126	0.124	0.114
Yb	2.08	1.06	1.35	0.81	0.86	0.83	0.81	0.82	0.75
Lu	0.319	0.165	0.199	0.121	0.13	0.125	0.124	0.117	0.113

TABLE 1. *(Cont.)*

Sample	WC04-03, 180.95-181.14	WC04-03, 192.67-192.81	WC04-03, 209.63-209.82	WC04-03, 244.38-244.61	WC04-03, 246.34-246.57	WC04-04, 9.37-9.48	WC04-04, 34.71-34.95	WCO4-04, 43.72-43.89	WC04-04, 63.14-63.29
Easting	591513	591513	591513	591513	591513	591517	591517	591517	591517
Northing	5350066	5350066	5350066	5350066	5350066	5349643	5349643	5349643	5349643
Drill hole	WC04-03	WC04-03	WC04-03	WC04-03	WC04-03	WC04-04	WC04-04	WCO4-04	WC04-04
Depth 2	180.95-181.14	192.67-192.81	209.63-209.82	244.38-244.61	246.34-246.57	9.37-9.48	34.71-34.95	43.72-43.89	63.14-63.29
Rock type 1	Quartz-feldspar porphyry	Quartz-feldspar porphyry	Quartz-feldspar porphyry	Quartz-feldspar porphyry	Quartz-feldspar porphyry	Feldspar porphyry	Feldspar porphyry	Feldspar porphyry	Feldspar porphyry
SiO_2 (wt %)	66.96	68.86	69.66	63.28	68.42	67.08	67.45	68.81	63.12
TiO_2	0.39	0.38	0.33	0.44	0.38	0.35	0.38	0.37	0.52
Al_2O_3	14.74	14.50	13.01	16.84	14.16	15.45	15.48	15.52	16.41
Fe_2O_3	3.50	3.65	3.52	4.17	4.73	3.60	3.40	3.21	5.61
MnO	0.040	0.046	0.036	0.034	0.032	0.021	0.025	0.026	0.031
MgO	1.46	1.53	1.24	1.83	1.41	1.28	1.30	1.36	2.29
CaO	2.84	2.31	2.97	3.61	2.32	2.43	2.67	2.67	3.57
Na_2O	5.01	4.84	3.87	2.19	4.72	4.69	4.65	4.74	3.92
K_2O	1.45	1.63	1.57	4.00	1.27	1.66	1.50	1.48	2.00
P_2O_5	0.13	0.12	0.09	0.11	0.11	0.09	0.10	0.09	0.15
LOI	2.39	2.57	2.75	6.30	2.48	2.76	2.33	2.04	3.29
Total	98.91	100.44	99.05	102.80	100.03	99.41	99.29	100.32	100.91
Ni (ppm)	17	11	13	14	11	7	7	9	21
Cr	8	<8	<8	13	12	16	<8	35	10
Co	9	8	9	15	11	14	11	9.00	20
V	42	44	48	61	47	50	52	38	66
Sc	3.3	3.5	3.3	5.4	3.6	3.5	4.5	3.6	4.6
Cu	593	697	404	34	314	940	294	583	1279
Zn	66	68	47	54	68	50	31	37	44
Cd	ND	ND	ND	ND	ND	ND	ND	ND	ND
Mo	ND	ND	ND	ND	ND	ND	10	ND	ND
W	3	ND	6	3	ND	7	12	14	ND
Nb (XRF)	4	3	3	3	4	5	5	6	5
Y (XRF)	10	10	7	8	10	11	11	10	11
Zr (XRF)	94	83	77	77	90	93	92	93	100
Zr	98.6	98.2	83.2	83.2	94.8	100	102.3	104.3	107.9
Hf	2.9	2.8	2.3	2.3	2.7	3	3.1	3	3
Nb	4.7	4.2	2.8	3.1	4.2	5.6	5.2	5.1	5.3
Ta	0.38	0.29	0.19	0.22	0.32	0.47	0.47	0.43	0.4
Y	7.55	7.64	4.34	5.92	6.99	7.92	8.92	7.11	8.48
Be	0.42	0.37	0.39	0.56	0.7	0.79	0.61	0.71	0.62
Li	11	12	9	12	12	11	9	10	14
Cs	0.817	0.891	0.879	1.845	1.016	1.324	0.954	0.942	1.479
Rb	40.82	42.18	52.85	108.94	37.9	51.1	43.2	45.09	76.73
Ba	264	257	175	300	266	392	244	306	306
Sr	183.2	112.5	150	54	190	257.4	243.4	237.4	252.9
Th	1.73	1.18	1.07	1.32	1.56	2.08	2.17	2.08	1.49
U	0.35	0.329	0.307	0.454	0.375	0.649	0.739	0.633	0.564
La	6.68	6.84	5.06	7.16	7.36	11.51	12.05	9.86	11.2
Ce	14.66	15.58	10.58	15.92	16.16	24.58	25.44	21.53	24.9
Pr	1.93	2.053	1.292	2.027	2.089	3.067	3.25	2.702	3.147
Nd	8.73	9.08	5.48	8.43	9.06	12.4	12.96	10.78	12.79
Sm	1.94	2.09	1.16	1.79	2	2.57	2.76	2.26	2.6
Eu	0.617	0.611	0.528	0.577	0.68	0.783	0.839	0.764	0.828
Gd	1.827	1.882	1.056	1.51	1.706	2.175	2.37	1.961	2.209
Tb	0.243	0.258	0.144	0.212	0.244	0.301	0.331	0.267	0.309
Dy	1.354	1.414	0.795	1.16	1.327	1.575	1.766	1.412	1.667
Ho	0.264	0.274	0.156	0.219	0.257	0.299	0.336	0.266	0.315
Er	0.734	0.747	0.451	0.61	0.717	0.831	0.938	0.754	0.871
Tm	0.104	0.11	0.068	0.084	0.103	0.122	0.138	0.113	0.127
Yb	0.69	0.7	0.44	0.54	0.68	0.83	0.9	0.75	0.82
Lu	0.105	0.102	0.07	0.08	0.101	0.125	0.135	0.113	0.124

Table 1. *(Cont.)*

| Sample	WC04-04, 102.07-102.23	WC04-04, 104.75-104.94	WC04-04, 139.65-139.85	WC04-04, 163.78-163.94	WC04-04, 191.62-191.88	WCO4-04, 192.17-192.30	WC04-08, 49.25-49.42	03SJP038-1
Easting	591517	591517	591517	591517	591517	591517	591510	592158
Northing	5349643	5349643	5349643	5349643	5349643	5349643	5350267	5350781
Drill hole	WC04-04	WC04-04	WC04-04	WC04-04	WC04-04	WCO4-04	WC04-08	-
Depth 2	102.07-102.23	104.75-104.94	139.65-139.85	163.78-163.94	191.62-191.88	192.17-192.30	49.25-49.42	-
Rock type 1	Amygdaloidal andesite (dike?)	Amygdaloidal andesite (dike?)	Feldspar porphyry	Feldspar porphyry	Feldspar porphyry	Feldspar porphyry	Feldspar porphyry	Dacite porphyry
SiO_2 (wt%)	60.19	60.65	67.89	77.54	58.70	63.80	66.70	60.63
TiO_2	0.41	0.40	0.44	0.29	0.40	0.39	0.40	0.69
Al_2O_3	15.75	15.48	15.00	10.13	15.53	14.10	16.21	17.19
Fe_2O_3	3.84	3.19	3.12	3.16	3.40	3.72	2.53	5.56
MnO	0.136	0.124	0.025	0.018	0.120	0.032	0.038	0.09
MgO	1.97	1.58	1.64	1.25	1.92	1.53	1.44	2.68
CaO	5.41	5.12	2.24	1.82	6.09	4.00	2.16	6.71
Na_2O	1.32	0.97	5.00	3.08	2.10	4.17	6.21	2.36
K_2O	3.94	4.13	1.78	1.08	3.19	2.01	1.19	1.47
P_2O_5	0.13	0.12	0.11	0.09	0.10	0.11	0.11	0.19
LOI	7.85	7.22	2.14	2.19	7.17	5.13	2.51	2.73
Total	100.95	98.98	99.39	100.65	98.72	98.99	99.50	100.28
Ni (ppm)	34	17	15	17	23	14	6	36
Cr	12	14	11	<8	15	17	<8	30.01
Co	29	11	11	16	14.00	16.00	4.00	19
V	65	64	37	30	63	50	51	86.8
Sc	4.6	4.4		3.1	4.6	3.6	3.8	6.2
Cu	20	98		1017	N.D.	2446	621	301
Zn	346	94		30	186	58	79	84
Cd	ND	ND		ND	ND	ND	ND	ND
Mo	ND	ND		ND	ND	400	ND	ND
W	11	12		11	3	10	ND	5
Nb (XRF)	3	3	3	3	2	1	3	9
Y (XRF)	7	8	10	6	8	11	9	9
Zr (XRF)	78	77	92	47	77	90	97	114
Zr	86.7	84	99.6	57.7	82.8	88.9	109.8	118.8
Hf	2.3	2.3	2.7	1.6	2.2	2.5	3	3.3
Nb	3.3	3.3	4.4	2.9	3.2	4.8	3.8	8.2
Ta	0.28	0.24	0.29	0.19	0.22	0.34	0.27	0.57
Y	5.14	5.31	7.88	4.38	5.91	8.67	6.94	8.86
Be	0.5	0.49		0.45	0.47	0.49	0.75	0.47
Li	6	5		10	18	13	13	12
Cs	2.704	2.903	0.979	0.602	2.238	0.991	1.172	0.906
Rb	117.05	122.82	58.79	36.36	104.74	52.45	43.01	50.04
Ba	269	254		131	291	214	124	384
Sr	61.8	58.1	160.9	129.8	105.8	165.8	154.4	275.3
Th	1.45	1.46	1.51	0.9	1.36	1.78	1.55	1.65
U	0.474	0.524	0.574	0.391	0.455	0.41	0.565	0.476
La	10.39	10.56	10.14	4.76	8.51	16.56	8.5	13.5
Ce	21.94	22.42	23.7	10.94	18.8	34.31	19.7	29.22
Pr	2.731	2.838	3.134	1.462	2.352	4.101	2.554	3.57
Nd	10.88	11.17	13.13	6.05	9.57	16.82	10.61	14.09
Sm	1.98	2	2.65	1.29	2.05	3.24	2.19	2.78
Eu	0.494	0.604	0.799	0.475	0.713	0.771	0.556	0.875
Gd	1.517	1.59	2.272	1.124	1.701	2.615	1.786	2.36
Tb	0.202	0.2	0.3	0.155	0.23	0.338	0.235	0.324
Dy	1.008	1.038	1.543	0.856	1.157	1.779	1.295	1.792
Ho	0.191	0.192	0.294	0.163	0.215	0.33	0.251	0.341
Er	0.531	0.54	0.822	0.477	0.565	0.906	0.717	0.945
Tm	0.076	0.077	0.113	0.068	0.079	0.127	0.104	0.135
Yb	0.49	0.51	0.93	0.44	0.51	0.81	0.72	0.87
Lu	0.072	0.076	0.113	0.067	0.075	0.128	0.109	0.128
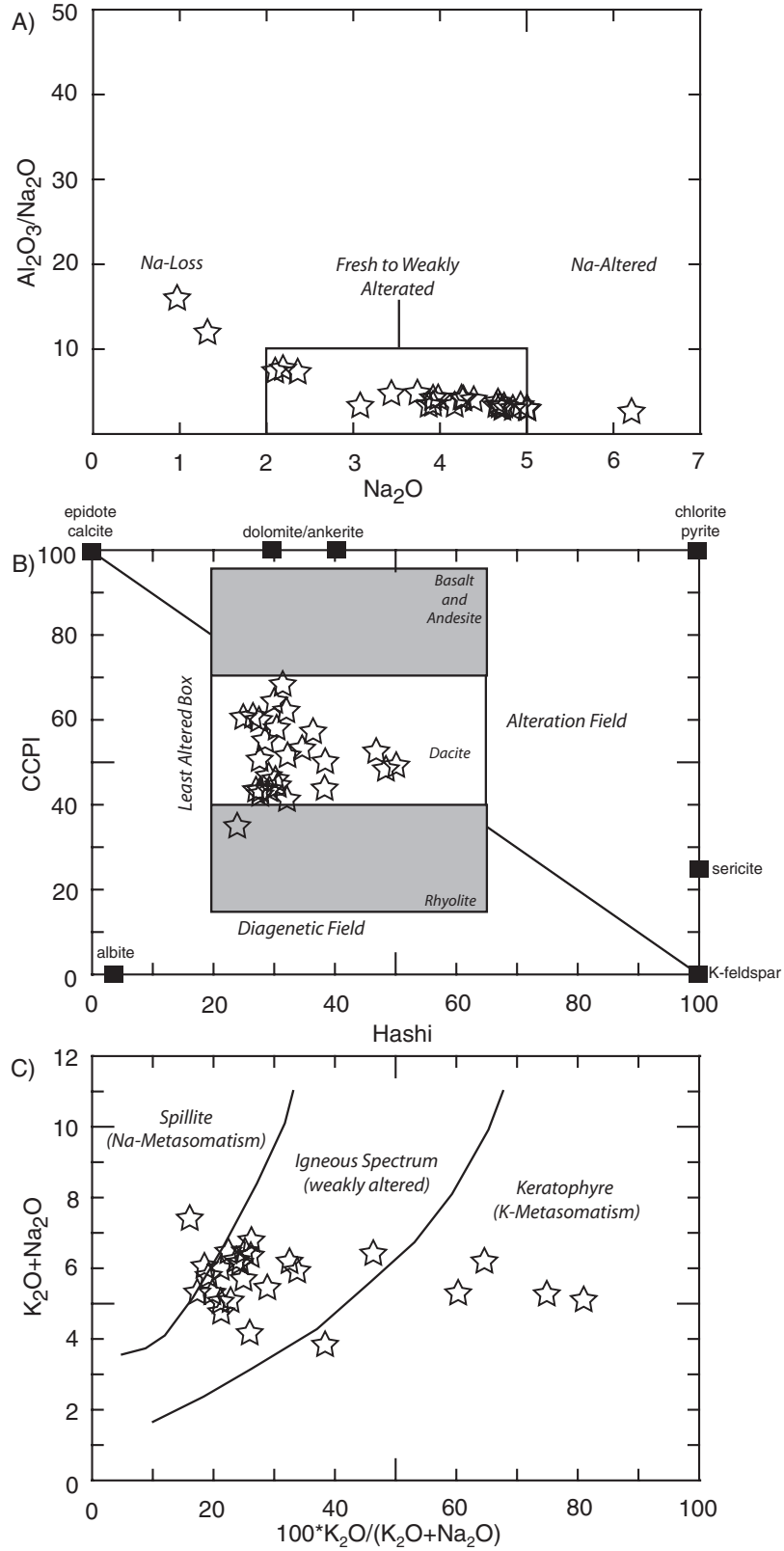
FIG. 7. Major element alteration plots for the rock of the Clifford intrusive suite, including: (A) an Al_2O_3/Na_2O-Na_2O plot with designations for least altered samples (Al_2O_3/Na_2O index from Spitz and Darling, 1978), (B) alteration box plot from Large et al. (2001) with Hashimoto alteration (Saeki and Date, 1980; Date et al., 1983) plotted against chlorite-carbonate-pyrite index [CCPI: $(MgO + Fe_2O_{3(total)})/(MgO + Fe_2O_{3(total)} + Na_2O + CaO)$], and (C) $(K_2O + Na_2O)$-$(100°K_2O/K_2O + Na_2O)$ plot of Hughes (1973).
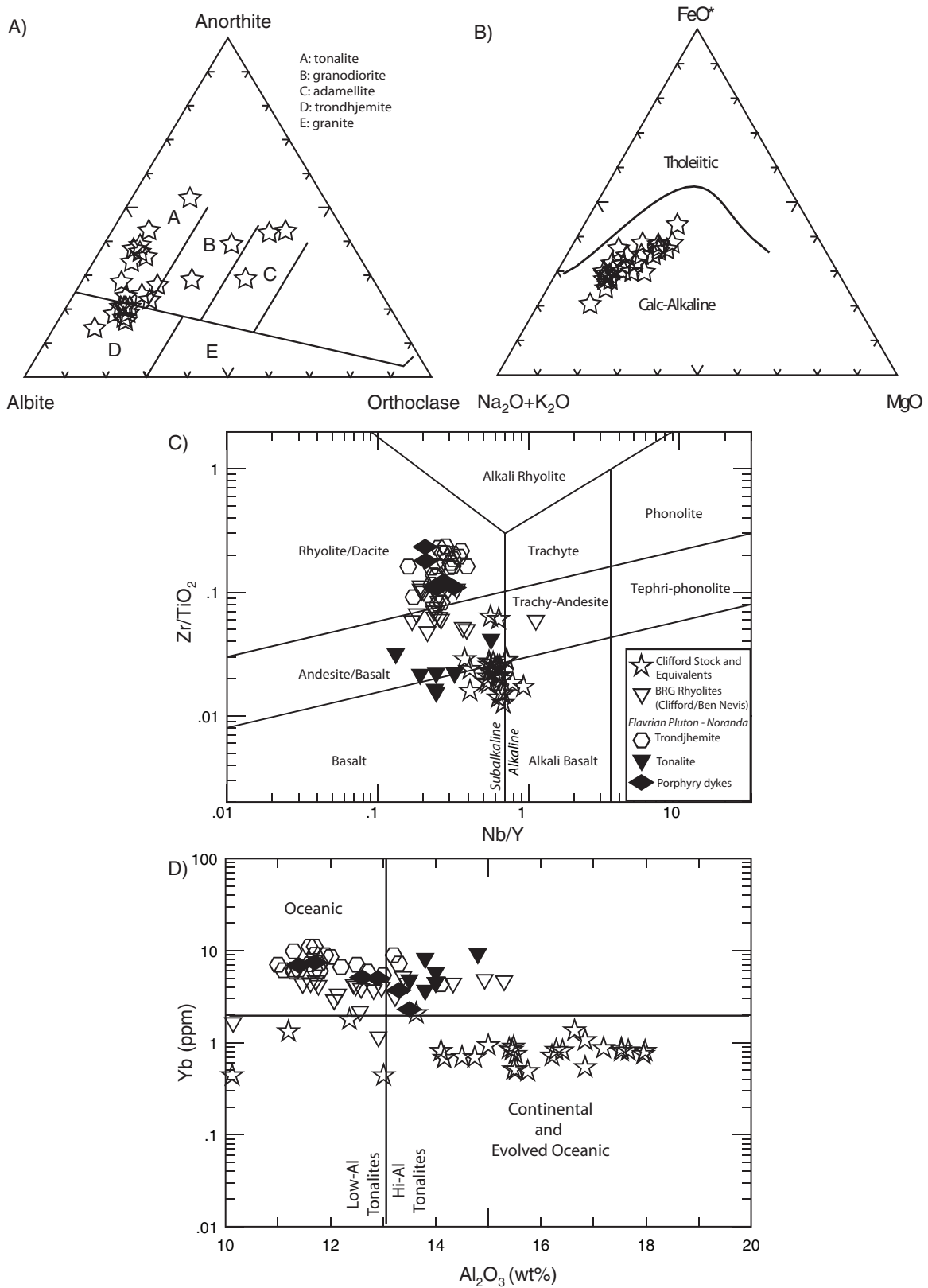
FIG. 8. Classification plots for the rocks of the Clifford stock intrusive suite. A. Normative feldspar diagram from O'Connor (1965). B. AFM plot from Irvine and Baragar (1971). C. Modified Winchester and Floyd (1977) Zr/TiO_2-Nb/Y discrimination diagram (from Pearce, 1996). D. Al_2O_3-Yb diagram for classifying different types of TTG from Arth (1979). Data for the Flavrian-Powell intrusive complex from Galley et al. (2002) and Galley (2003). Data for Blake River Group rhyolites from Ontario from Péloquin and Piercey (2005).
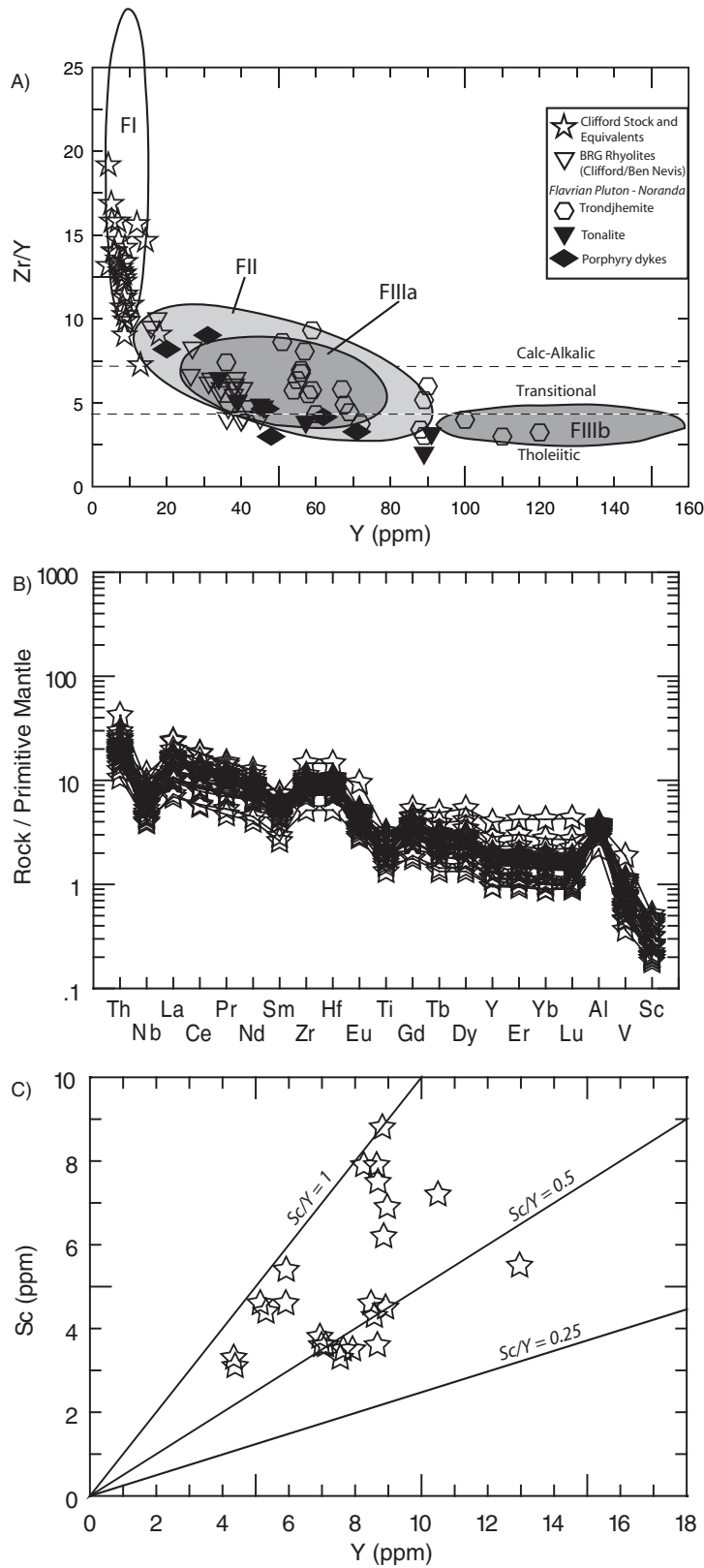
FIG. 9. Trace element plots for rocks of the Clifford stock and equivalents. A. Zr/Y-Y diagram of Lesher et al. (1986) as modified by Lentz (1998), with magmatic affinities based on Zr/Y ratios from the concepts of Barrett and MacLean (1999). B. Primitive mantle normalized plot. C. Sc-Y plot of Feng and Kerrich (1992). Data for the Flavrian-Powell intrusive complex from Galley et al. (2002) and Galley (2003). Data for Blake River Group rhyolites from Ontario from Péloquin and Piercey (2005).
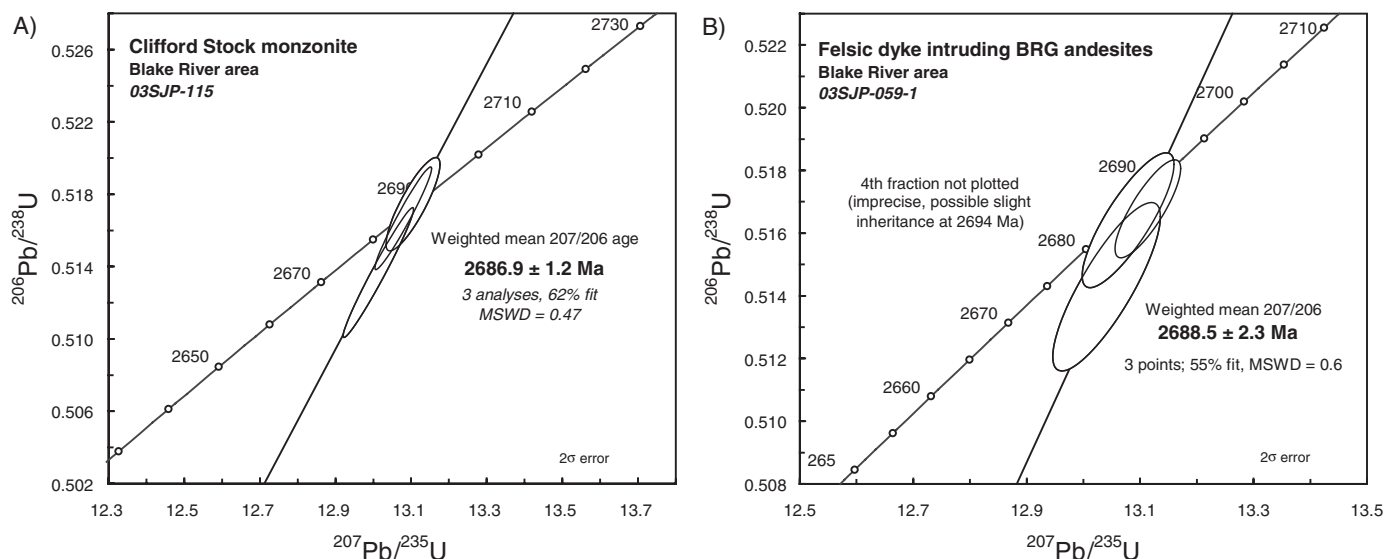
FIG. 10. Concordia diagrams showing Pb-U isotope data for samples of the Clifford stock (A) and associated dike (B).

and are interpreted to be younger than the surrounding rocks of the Blake River Group. In drill core, porphyry dikes have sharp contacts with surrounding rocks, supporting a postvolcanic origin. Abundant, high-quality zircons were recovered from this sample, comprising populations of colorless to pale brown, water-clear, euhedral long prisms, and stubbier or lozenge-shaped, sharp, doubly terminated grains. Small fluid, melt, or apatite inclusions were present in most zircons, but their abundance was minor. Four representative single grains were abraded and analyzed. All analyses are overlapping and are less than 0.6 percent discordant. Precise analyses obtained for the three most concordant fractions (A1, A3, A4) yield a weighted mean $^{207}Pb/^{206}Pb$ age of 2688.5 ± 2.3 Ma (±7.2 Ma including decay constant uncertainty; Fig. 10, Table 2). The fourth fraction (A2) has a high proportion of common Pb and commensurate large errors, and yields a slightly higher $^{207}Pb/^{206}Pb$ age (2694 ± 5 Ma), which may reflect minor inheritance (Fig. 10, Table 2). The age of inheritance is similar to ages for the Blake River Group regionally (Corfu et al., 1989; Mortensen, 1993; Galley and van Breemen, 2002).

The 2688.5 ± 2.3 Ma age is the best estimate of the timing of emplacement and crystallization of the felsic dike. This age is similar to the Clifford stock and suggests that the dikes are coeval with the stock, consistent with the lithogeochemical results. Moreover, these ages are synchronous with late-tectonic magmatic activity throughout the eastern Abitibi (Table 3; Corfu et al., 1989; Corfu and Noble, 1992; Mortensen, 1993).

Re-Os Geochronology

Two samples of porphyry with gray quartz veins with Cu-Mo-Au mineralization were sampled to test the age of porphyry-style mineralization associated with the Clifford stock and associated dikes. The two samples were processed to separate molybdenite following the methods presented by Selby and Creaser (2004). Sample WC04-03-195 contained a centimeter-sized quartz vein cutting across a feldspar porphyry host rock. Small molybdenite-rich patches and veinlets within the quartz vein were present. Sample WC04-05-146 contained a single thin (~5 mm) stockwork vein with visible molybdenite and some pyrite. For both samples, the vein material was cut away from the host rock and molybdenite separated by metal-free crushing, gravity, magnetic, and water-floatation methods. The ^{187}Re and ^{187}Os concentrations in molybdenite were determined by isotope dilution mass spectrometry at the University of Alberta Radiogenic Isotope Facility, following the methodology of Selby and Creaser (2001a, b, 2004). Results are presented in Table 4 and, for both samples, identical Re-Os model ages are calculated. Both samples of molybdenite have similar high Re contents (~250 ppm), which is common for molybdenite associated with porphyry-style Cu-Mo deposits. The model ages of 2681 ± 7 and 2684 ± 7 Ma overlap within analytical uncertainty, and a weighted average of 2682.4 ± 5 Ma (±7.8 Ma including decay constant uncertainty) provides the best determination of molybdenite formation in the veins (Table 4). These values, although younger, are within uncertainty of the U-Pb ages of the host porphyry dikes.

Discussion

The Blake River Group in Ontario has an episodic metallogenic history with early VMS-related activity overprinted by younger porphyry Cu-Mo-Au mineralization. The older VMS-style alteration includes both epidote-quartz-(chlorite)-pyrite alteration as infillings in amygdules within basaltic rocks and chlorite-quartz-chalcopyrite alteration and mineralization. Other occurrences, such as the Canagau showing, are also considered to represent synvolcanic mineralization (Jensen, 1975; Hannington et al., 2003). The age of the synvolcanic hydrothermal alteration is constrained to be between 2699.8 ± 3.6 Ma, the age for a synvolcanic rhyolite dike that cuts mineralization but is likely synchronous with the altered basalts and 2696.6 ± 1.3 Ma, the age for rhyolite from the Pb-Ag–rich Canagau occurrence (Péloquin and Piercey, 2005; Péloquin et al., 2008). Thus, VMS-style mineralization in the Blake River Group in Ontario is similar in age to other VMS

TABLE 2. U–Pb Isotope Data for Zircon from the Clifford Stock and Associated Dike

Sample Fraction	Analysis no.	Description	Weight (mg)	U (ppm)	Th/U	Pb* (pg)	Pbc (pg)	^{206}Pb/^{204}Pb	^{206}Pb/^{238}U	± 2σ	^{207}Pb/^{235}U	± 2σ	^{207}Pb/^{206}Pb	± 2σ	^{207}Pb/^{206}Pb Age (Ma)	± 2σ	Disc. (%)	Corr. Coeff.
03SJP-115-1		Clifford Stock monzogranite, Clifford Twp.																
Z1	MAH4010	1 cls-pbr, clr, elong euh prism (>4:1); minor incl	0.0025	141	0.48	207.3	2.2	5337	0.51364	0.00292	13.0176	0.0758	0.18381	0.00023	2687.6	2.1	0.7	0.9770
Z2	MAH4007	1 large, pbr, clr, frag; minor incl, frac	0.0008	147	1.02	74.0	2.1	1796	0.51737	0.00209	13.1081	0.0576	0.18375	0.00043	2687.0	3.9	0.0	0.8507
Z3	MAH4012	1 large, cls, clr, frag; minor incl, frac	0.0014	102	0.51	85.8	1.2	4154	0.51660	0.00230	13.0819	0.0612	0.18366	0.00022	2686.2	2.0	0.1	0.9668
03SJP-059-1		Feldspar-phyric dike, Clifford Twp.																
A1	MAH4025	1 large, cls-pbr, faceted lozenge; incl	0.0054	75	0.42	234.3	9.3	1462	0.51674	0.00126	13.1129	0.0471	0.18405	0.00039	2689.7	3.5	0.2	0.8212
A2	MAH4026	1 large, cls-pbr, faceted lozenge or frag; incl	0.0091	28	0.40	161.5	21.9	375	0.51799	0.00784	13.1813	0.2331	0.18456	0.00118	2694.3	10.5	0.2	0.9362
A3	MAH4027	1 large, pbr, faceted lozenge; incl	0.0075	38	0.45	163.8	9.8	975	0.51638	0.00174	13.0777	0.0663	0.18368	0.00054	2686.4	4.9	0.1	0.8281
A4	MAH4056r	1 large, pbr, faceted lozenge; incl	0.0133	33	0.40	250.6	17.4	848	0.51429	0.00218	13.0406	0.0779	0.18390	0.00062	2688.4	5.6	0.6	0.8317

Notes: All analyzed fractions represent least magnetic, air-abraded single zircon grains, free of inclusions, cores or cracks, unless otherwise noted; abbreviations: clr = clear, cls = colorless, elong = elongate, euh = euhedral, frac. = fracture(s), frag = fragment, incl = inclusions, pbr = pale brown, prism = prismatic; Pb* is total amount (in pg) of radiogenic Pb; Pbc is total measured common Pb (in pg) assuming the isotopic composition of laboratory blank: 206/204 = 18.221; 207/204 = 15.612; 208/204 = 39.360 (errors of 2%) Pb/U atomic ratios are corrected for spike, fractionation, blank, and, where necessary, initial common Pb; ^{206}Pb/^{204}Pb is corrected for spike and fractionation; Th/U is model value calculated from radiogenic ^{208}Pb/^{206}Pb ratio and ^{207}Pb/^{206}Pb age assuming concordance; Disc. (%) percent discordance for the given ^{207}Pb/^{206}Pb age uranium decay constants are from Jaffey et al. (1971)

TABLE 3. Summary of Ages for Intrusions within the Blake River Group of Ontario and Québec and Intrusion-Associated Volcanics and Mineralization

Intrusion	Associated volcanic rocks	Age (Ma)	Assocated mineralization	References
Flavrian-Powell (early trondjhemite)	Lower Blake River Group (pre-Cauldron volcanics)	2700.8 +2.6/-1.0	Noranda Cu-Zn VMS deposits	Mortensen (1993)
Flavrian-Powell (late trondjhemite	Lower Blake River Group (pre-Cauldron volcanics)	2700 +3/-2	Noranda Cu-Zn VMS deposits	Galley and van Breeman (2002)
Flavrian Powell (late aplite associated with St. Jude breccia pipe)	Upper Blake River Group (post-Cauldron volcanics (?))	2697 ± 2	Cu-Mo-Au breccia pipe (porphyry)	Galley and van Breeman (2002)
Clifford Township Blake River Group synvolcanic rhyolite dikes	Upper Blake River Group (Clifford and Ben Nevis Townships)	2699.8 ± 3.6 (Canagau rhyolite yielded 2696.6 ± 1.3)	Au-rich VMS occurrences (Canagau)	Peloquin and Piercey (2005) and Peloquin et al. (2008)
Mooshla pluton (oldest tonalite phase)	Upper Blake River Group (post-Cauldron volcanics (?))	2696 ± 3	Cu-Zn VMS, Au-rich VMS	Zhang and Machado (1993)
Mooshla pluton (feldspar-quartz porphyry)	Upper Blake River Group (post-Cauldron volcanics (?))	2696.9 ± 1	Cu-Zn VMS, Au-rich VMS	Lafrance et al. (2005)
Clericy granite	Upper Blake River Group (post-Cauldron volcanics (?))	2696 ± 1.5	Au-rich VMS (Mobrun deposit)	Mortensen (1993)
Clarice Lake Stock	-	2689 ± 1	-	Corfu and Noble (1992)
Lac Dufault Pluton	-	2690 ± 2	-	Mortensen (1993)
Clifford Stock and associated dikes	-	2686.9 ± 1.2 (Clifford stock), 2688.5 ± 2.3 (dykes), and 2682.4 ± 5 (Re-Os on molybdenite)	Cu-Mo-Au breccia pipe (porphyry) - Croxall	This study

TABLE 4. Re-Os Data for Molybdenite Separates from Porphyry Cu-Mo-Au Mineralization from Clifford Township

Sample no.	Re (ppm)	±2σ	^{187}Os (ppb)	±2σ	^{187}Os/^{187}Re	Model age	±2σ	±2σ with decay constant uncertainties
WC0405-146	256.6	0.6	7366	10	0.04568	2681	7	11
WC0403-195	219.4	0.5	6304	9	0.04572	2684	7	11

mineralization in the Blake River Group (Mortensen, 1993; Galley and van Breemen, 2002; Lafrance et al., 2005).

In contrast, the porphyry Cu-Mo-Au mineralization is a distinctly younger event unrelated to sea-floor hydrothermal activity. Porphyry Cu-Mo-Au veins cut the Clifford stock and equivalent dikes that have yielded U-Pb dates of 2686.9 ± 1.2 and 2688.5 ± 2.3 Ma, respectively (Fig. 10, Table 2). Furthermore, Re-Os isotope data for molybdenite separates from these veins yield a weighted average age of 2682.4 ± 5.0 Ma age (±7.8 with decay constant uncertainties; Table 4). Although this Re-Os age is slightly younger than the U-Pb ages for the Clifford stock and associated dikes, it is within uncertainty of the U-Pb ages for this intrusive activity. Given the magmatic metal signature of the mineralization and the absence of similar aged magmatic rocks elsewhere in the region, it is reasonable to assume that the mineralization was synchronous with the Clifford stock.

The late-stage porphyry Cu-Mo-Au mineralization found in this study represents a slightly younger, previously unrecognized episode of hydrothermal activity in the Blake River Group. Overprinting porphyry Cu-Mo-Au mineralization is found in numerous VMS camps (Galley et al., 2000; Galley and van Breemen, 2002), and Cu-Mo-Au mineralization is found in the late phases of the Flavrian pluton (e.g., St. Jude breccia), coincident with postcauldron magmatism and Au-rich VMS deposit formation (Galley and van Breemen, 2002). The ~2689 to 2686 Ma porphyry Cu-Mo-Au mineralization in Clifford Township, however, is unique in that it is associated with a plutonic event that is not associated with voluminous, coincident volcanic activity, as in other VMS districts (Table 3).

This late-stage magmatic event at ~2690 to 2685 Ma is widespread across the entire Blake River Group and Abitibi subprovince (Corfu et al., 1989; Corfu and Noble, 1992; Mortensen, 1993; Ayer et al., 2002) and suggests the potential for other plutons of this age to host Cu-Mo-Au mineralization.

In the absence of precise geochronology, it is important to distinguish between potentially synvolcanic plutons and later phases of intrusive activity that are unlikely to have driven VMS-producing hydrothermal systems (Galley, 2003).

Previous studies have assumed that the Clifford stock was co-eval with the Blake River Group and the Flavrian-Powell Intrusive Complex. The new U-Pb zircon geochronology indicates that it represents a distinctly younger phase of igneous activity (~2690–2686 Ma) occurring ~5 to 10 m.y. after the youngest phase of igneous activity in the Blake River Group and Flavrian-Powell intrusive complex (Mortensen, 1993; Galley and van Breemen, 2002; Lafrance et al., 2005;). In addition, mapping shows that the Clifford intrusive suite is not associated with abundant, coeval volcanic rocks, it is not a polyphase intrusive system, it has limited areal extent (less than 5 km² in comparison to the Flavrian-Powell intrusive complex which has an extent of at least 50 km²), and it is associated with only porphyry-style Cu-Mo-Au mineralization.

The Clifford stock is also geochemically distinct from the Flavrian-Powell intrusive complex. It has higher Al_2O_3 contents, distinctively lower Y, Yb, Th, and HFSE, higher Zr/Y, La/Yb, Sm/Yb, and Al_2O_3/Yb ratios, and lower Zr/Nb, Zr/Th, Zr/La, and Zr/TiO_2 relative to the Flavrian-Powell intrusive complex (Figs. 8, 9, 11). These differences can be explained

by two processes: variations in the depth of melting and variations in the temperatures of melting and emplacement.

Origin of the intrusive rocks

The difference in degree and depth of partial melting is evident from the variable Y, Yb, and associated ratios (Zr/Y, La/Yb, Sm/Yb, and Al_2O_3/Yb) between the Clifford intrusive suite and the Flavrian-Powell intrusive complex. These differences can be modeled by assuming that the source regions for both suites were basaltic in composition and by varying the residual mineralogy as a function of the depth of melt generation (e.g., eclogite, garnet amphibolite, and amphibolite; Fig. 12). Basalt with enriched mid-ocean ridge basalt (E-MORB) composition from the Blake River Group has been chosen as the starting material for the melt models (data from MacDonald et al., 2005). This source composition was chosen as it is a common substrate underlying the Blake River Group in Ontario and Quebec (Lafleche et al., 1992a, b; MacDonald and Piercey, 2003) and is consistent with sources chosen for similar models by other workers (e.g., Rapp et al., 1991; Rapp
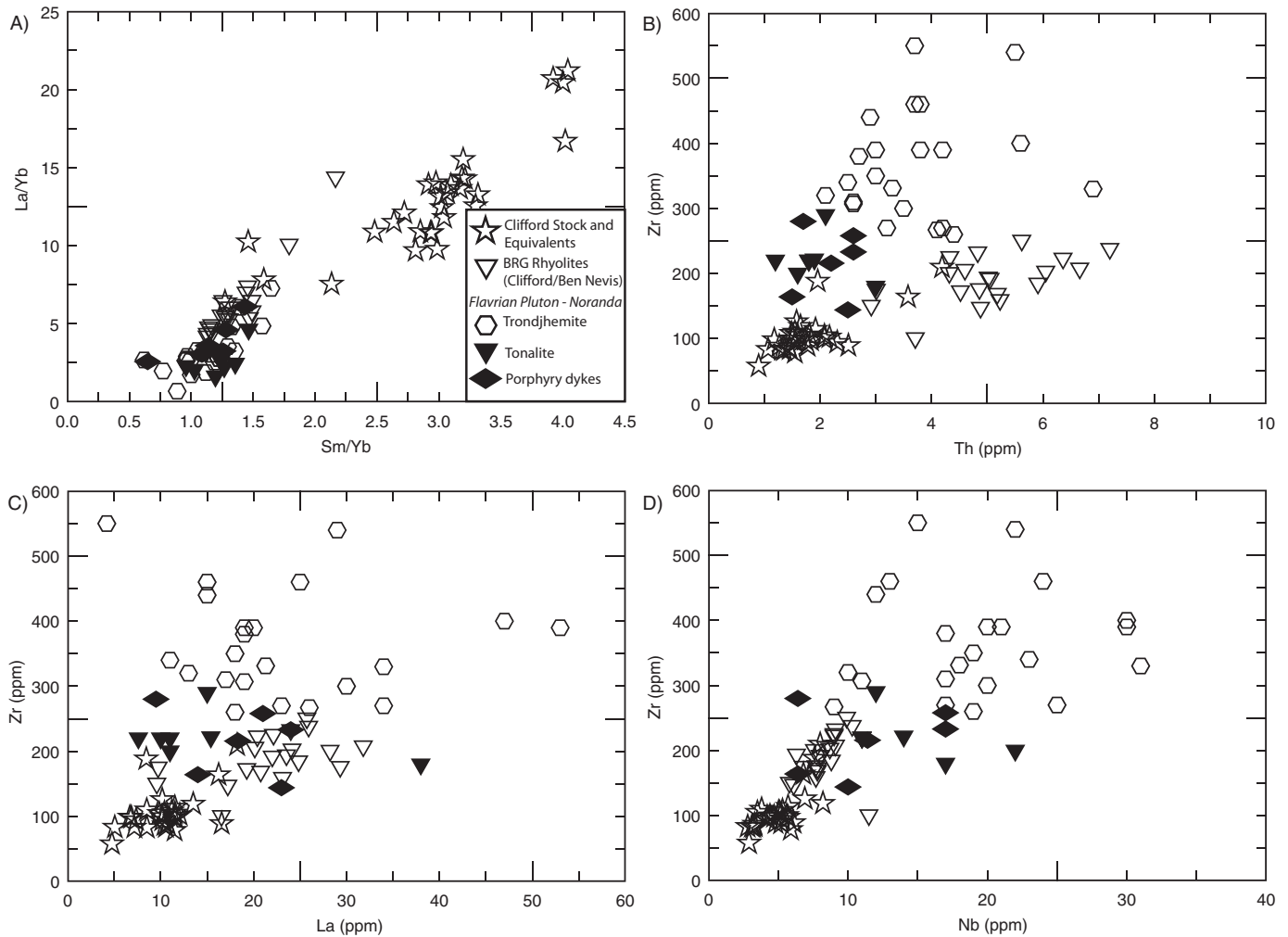
Fig. 11. Trace element diagrams illustrating differences between the Clifford intrusive suite and the Flavrian-Powell intrusive complex. A. La/Yb-Sm/Yb. B. Zr-Th. C. Zr-La. D. Zr-Nb. Data for the Flavrian-Powell intrusive complex from Galley et al. (2002) and Galley (2003). Data for Blake River Group rhyolites from Ontario from Péloquin and Piercey (2005).
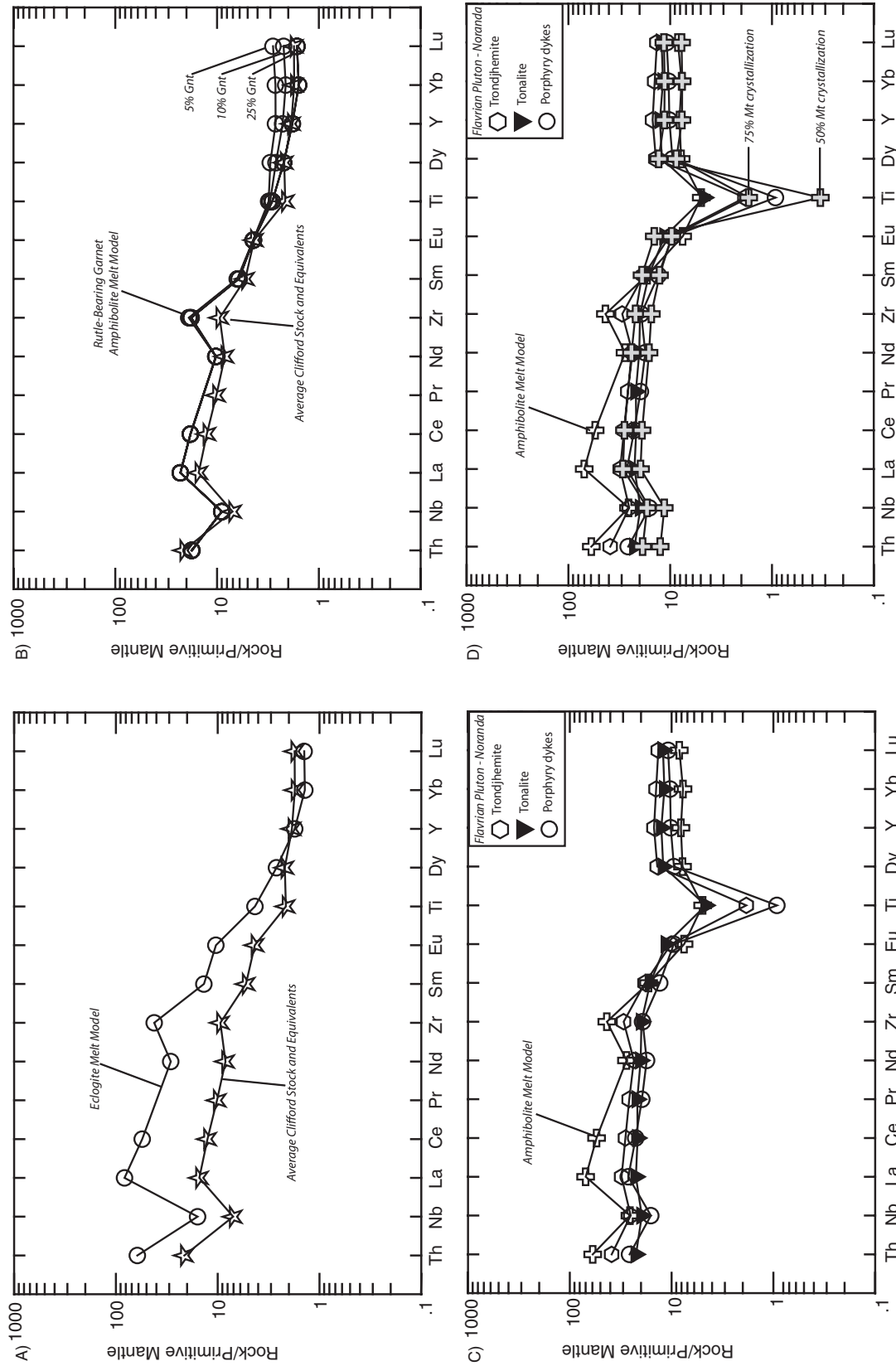
FIG. 12. Trace element models for amphibolite melting using an amphibolite with E-MORB chemistry and different residual mineral phases. Varying residual mineral phases were chosen to represent variations in the depth at which melting occurred (e.g., eclogite, garnet amphibolite, and amphibolite). Shown in (A) and (B) is the average composition of the Clifford intrusive suite; in (C) and (D) are the average tonalite, trondhemite, and porphyry dikes from the Flavrian complex (data from Galley et al., 2002). Melt models in (A) to (D) are 10 percent partial melts. Partition coefficient for REE are from Cousens et al. (2002); partition coefficients for all other elements are from Bedard (2006). The starting E-MORB composition is an average E-MORB from the Blake River Group in Ontario (from MacDonald et al., 2005). A. An eclogite partial melt model (modal proportions from Bedard, 2006) illustrates that an eclogitic restite creates a melt model enriched in LREE and depleted in HREE relative to the Clifford stock. B. A rutile-bearing garnet amphibolite melt model (with curves representing 5, 10, and 25% garnet; modal proportions for the restite as in Cousens et al., 2002) is similar to the Clifford stock. C. An ilmenite-bearing amphibolite partial melt model (modal proportions for the restite from Cousens et al., 2002) for the Flavrian intrusive complex provides signatures that are similar to the Flavrian complex but slightly elevated in LREE and not sufficiently depleted in Ti. Subsequent crystallization of magnetite from the melt, however, successfully reproduces the signatures of the Flavrian intrusive complex rocks (D). Data for the Flavrian complex from Galley et al. (2002).

and Watson, 1995; Bedard, 2006; Moyen and Stevens, 2006). Other sources were tested (e.g., arc tholeiite and crustally contaminated MORB), but the Nb-Th-La relationships and REE characteristics of the Clifford intrusive suite and Flavrian-Powell intrusive complex could not be replicated using these sources.

Models for TTG petrogenesis typically invoke deep melting of basalt with eclogitic residues, either via slab melting or delamination, or shallower melting with garnet granulite or amphibolitic residues (Drummond and Defant, 1990; Rapp et al., 1991; Rapp and Watson, 1995; Drummond et al., 1996; Martin et al., 2005; Bedard, 2006; Moyen and Stevens, 2006). The eclogite residue has been chosen by many workers because it explains the heavy REE (HREE) depletion (the HREE are sequestered by the residual garnet) and the negative primitive mantle normalized Ti-Nb-Ta anomalies present within TTG suite rocks (Ti-Nb-Ta are sequestered in rutile within the eclogite). A model using an eclogite residue yields results that are too depleted in HREE and too enriched in highly incompatible elements to be the analog of the Clifford intrusive suite (Fig. 12), so they cannot be the products of deep melting, such as melting of the subducted slab (Drummond and Defant, 1990; Drummond et al., 1996). The trace element signatures of the Clifford intrusive suite can be modeled successfully, however, using a rutile-bearing garnet amphibolitic residue. In contrast, the Flavrian-Powell intrusive complex is best modeled by an ilmenite-bearing amphibolitic residue coupled with fractional crystallization of magnetite (Fig. 12).

The modeled residues for the Clifford intrusive suite and Flavrian-Powell intrusive complex are consistent with different depths and pressures of melt generation. Using temperatures consistent with melting temperatures for TTG (e.g., 750°–1,000°C), melts with amphibolitic residual mineralogy would likely have formed within the upper 40 km of Earth's surface (Fig. 13; e.g., Rapp et al., 1991; Wolf and Wyllie, 1994; Rapp and Watson, 1995; Wyllie et al., 1997; Moyen and Stevens, 2006;). In contrast, melts with garnet amphibolite residues would have formed at depths greater than 40 km,

whereas eclogitic residues would occur at even greater depths (>50–60 km; e.g., Rapp et al., 1991; Wolf and Wyllie, 1994; Rapp and Watson, 1995; Wyllie et al., 1997; Moyen and Stevens, 2006). The models presented herein support the assertion that the Clifford intrusive suite was generated where garnet was a stable in the residue at great depths, whereas the Flavrian-Powell intrusive complex was generated where garnet was not stable in the residue and, therefore, at shallower depths (Fig. 14).

However, the absolute differences in HFSE and REE (and Zr/TiO_2 ratios) abundances between the Clifford intrusive suite and the Flavrian-Powell intrusive complex (Figs. 8, 9, 11) cannot be explained entirely by differences in depth and degree of partial melting. The Flavrian-Powell intrusive complex has consistently higher HFSE and REE contents when compared to the Clifford intrusive suite, a feature that can be attributed to variations in the melting temperatures at which the different suites were generated. Abundant experimental and empirical work has shown that for felsic rocks the higher the temperature of melt generation, the greater the HFSE and REE content of the felsic melts (Watson and Harrison, 1983; Clemens et al., 1986; Skjerlie and Johnston, 1992; Bea, 1996a, b; Watson, 1996; Chappell et al., 2000; King et al., 2001), consistent with the Flavrian-Powell intrusive complex being generated at higher temperatures than the Clifford intrusive suite.

Zircon saturation temperatures also support a higher temperature origin for the Flavrian-Powell intrusive complex. Zircon saturation temperatures are calculated using the equation of Watson and Harrison (1983):

$$ln\ D^{Zr,\ zircon/melt} = [-3.8 - [0.85(M-1)]] + 12,900/T, \quad (1)$$

where $D^{Zr,\ zircon/melt}$ is the ratio of Zr concentration (ppm) in zircon to that in a saturated melt (i.e., the mineral-melt partition coefficient for Zr in zircon from Watson and Harrison (1983), M is the alumina saturation factor for the rock [M = $(Na + K + 2 \cdot Ca)/(Al \cdot Si)$], and T is temperature in Kelvin.
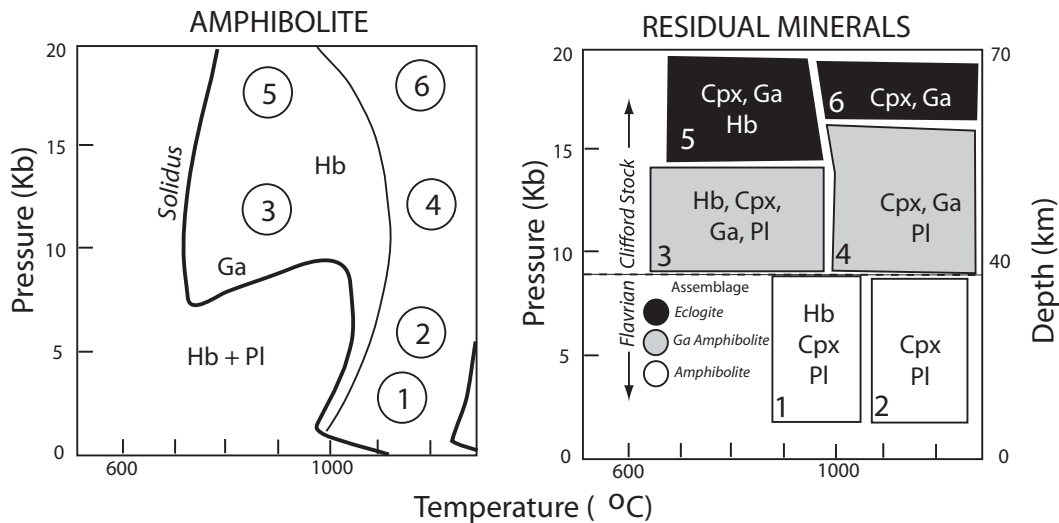

FIG. 13. Histograms of zircon saturation temperatures (TZrSat) for the Clifford intrusive complex (A) and the Flavrian-Powell intrusive complex (B). Data for the Clifford stock and equivalents from this study. Data for the Flavrian complex from Galley et al. (2002).
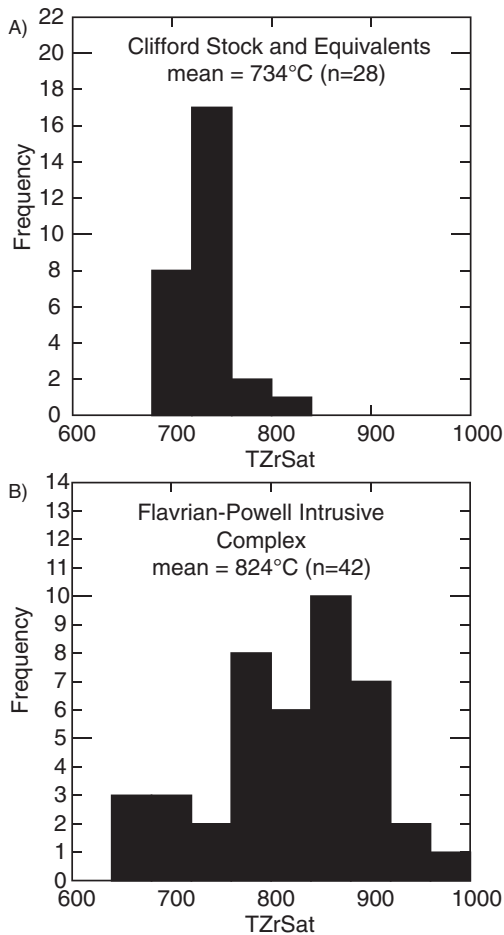
FIG. 14. A. Phase diagram for tonalite-trondjhemite formation via dehydration melting of amphibolite (modified after Wyllie et al., 1997). Numbers correspond to residual minerals present in the source during melting. B. Residual mineral phases present in the restite as a function of pressure and temperature. The trace element modeling results in Figure 12 suggest that the Clifford stock intrusive complex was generated at depths >40 km, whereas the Flavrian intrusive complex formed at shallower depths <40 km.

For rocks that do not have significant inherited zircon, like those in this study, zircon saturation temperatures provide minimum estimates of the temperature of the felsic rock at the source (Miller et al., 2003) and thereby provide an estimate of the temperature of formation of the felsic rock (e.g., Barrie, 1995). The Flavrian-Powell intrusive complex has an average zircon saturation temperature of 834ºC, whereas the Clifford intrusive suite has an average of 740ºC, supporting the inferred temperature differences based on HFSE-REE systematics (Fig. 13).

The different geologic and petrological attributes of the Flavrian-Powell intrusive complex and the Clifford intrusive suite may explain the different metallogenic histories of the two intrusive suites. Both intrusive complexes are spatially associated with mineralization, but there are significant differences in the associated metal endowment. The Flavrian-Powell intrusive complex was associated with ~110 Mt of mined ore (Galley, 2003), whereas the Clifford intrusive suite is associated with only minor Cu-Mo-Au occurrences. In contrast to the Clifford stock, the Flavrian-Powell intrusive complex is

a large, high-temperature intrusive complex generated and emplaced at a shallow level in the crust and therefore was able to drive robust and long-lived VMS-related hydrothermal systems (Cathles, 1981; Galley, 1996, 2003; Barrie et al., 1999a, b). Mineralogical and O isotope evidence in rocks surrounding the Flavrian-Powell intrusive complex illustrate that there was abundant high-temperature water-rock interaction and a robust hydrothermal system generated by this intrusive system (Cathles, 1993; Paradis et al., 1993; Taylor et al., 2000; Hannington et al., 2003a). In contrast, the Clifford stock and associated dikes are younger than the surrounding volcanic rocks and they exhibit evidence for generation at depth (i.e., low Y and Yb in the garnet stability field) and from lower temperature melts (Fig. 13). Oxygen isotope and mineral chemical evidence suggests that the hydrothermal system generated on a regional scale by the Clifford stock was cooler than that generated by the Flavrian-Powell intrusive complex (Taylor et al., 2000; Hannington et al., 2003a). The lack of significant VMS mineralization associated with the Clifford intrusive suite may be due to the fact that the subvolcanic intrusive system was generated at too great a depth, was of insufficient volume, and had too low a temperature of emplacement.

The Clifford stock and associated rocks, however, are associated with porphyry Cu-Mo-Au mineralization and have some geochemical attributes (e.g., adakitelike high La/Yb, low Y and Yb) that are similar to many Phanerozoic porphyry intrusions (e.g., Kay and Mpodozis, 2001; Borisova et al., 2006). It is possible that such late porphyries within the Abitibi greenstone belt could host significant Cu-Mo-Au mineralization.

Conclusions

Intrusive rocks associated with the Blake River Group in Ontario have characteristics that contrast significantly with those that host significant VMS mineralization in the eastern part of the group in the Noranda and Bousquet-LaRonde camps. In Ontario, intrusions are younger (2686.9 ± 1.2 and 2688.5 ± 2.3 Ma), have insignificant accumulations of VMS mineralization, are associated with porphyry Cu-Mo-Au mineralization (Re-Os molybenite ages of 2682.4 ± 5 Ma), are areally restricted, and not polyphase in nature. In comparison to the VMS-associated Flavrian-Powell intrusive complex in the Noranda camp, the western Blake River Group intrusions are characterized by lower total Y, Yb, Th, HFSE, and REE, with higher Zr/Y, La/Yb, Sm/Yb, Al_2O_3/Yb, and La/Sm$_{UCN}$ ratios, and lower Zr/Nb, Zr/Th, Zr/La, Zr/TiO$_2$, and Nb/Th$_{UCN}$ ratios. These characteristics are consistent with derivation from low-temperature melting (<800ºC) at depths >40 km in the crust where garnet is stable in the residue (e.g., garnet amphibolite residue). In contrast, the Flavrian-Powell intrusive complex is consistent with generation at shallow levels in the crust (i.e., <40-km depth) in the amphibolite stability field and at temperatures >800º to 850ºC. The occurrence of high-temperature magmatism at high levels within this crust that is coeval with volcanic activity explains the association of numerous VMS deposits with the Flavrian-Powell intrusive complex, as this intrusive complex would have generated abundant heat at high levels in the crust to drive hydrothermal circulation. In contrast, the western Blake River Group intrusions were generated at depth and at lower temperature

increasing the probability of heat loss upon emplacement from depth, thereby decreasing the probability of hydrothermal circulation at high levels in the crust and likely explaining the paucity of VMS mineralization with these intrusive rocks. The results presented herein build on previous studies and provide important lithogeochemical criteria for discriminating intrusions formed at depths that likely have less potential to produce VMS versus those formed at shallow levels with greater potential to drive hydrothermal circulation.

Whereas the intrusions of the western Blake River Group intrusions have limited VMS potential, they do have some geochemical characteristics that are similar to some Phanerozoic porphyry Cu-Mo-Au–associated intrusive systems, highlighting the potential of porphyry Cu-Mo-Au systems of Late Archean age elsewhere in the Abitibi.

Acknowledgments

REFERENCES

Arth, J.G., 1979, Some trace elements in trondhjemites—their implications to magma genesis and paleotectonic setting, *in* Barker, F., ed., Trondhjemites, dacites, and related rocks: New York, Elsevier, p. 123–132.

Ayer, J., Amelin, Y., Corfu, F., Kamo, S., Ketchum, J.F., Kwok, K., and Trowell, N.F., 2002, Evolution of the Abitibi greenstone belt based on U-Pb geochronology: autochthonous volcanic construction followed by plutonism, regional deformation and sedimentation: Precambrian Research, v. 115, p. 63–95.

Ayer, J.A., Thurston, P.C., Bateman, R., Dubé, B., Gibson, H.L., Hamilton, M.A., Hathway, B., Hocker, S.M., Houlé, M., Hudak, G., Lafrance, B., Lesher, C.M., Isopolatov, V., MacDonald, P., Péloquin, A.S., Piercey, S.J., Reed, L.H., and Thompson, P.H., 2005, Overview of results from the Greenstone Architecture Project: Discover Abitibi Initiative, Ontario Geological Survey Open File 6154, 146 p.

Barrett, T.J., and MacLean, W.H., 1999, Volcanic sequences, lithogeochemistry, and hydrothermal alteration in some bimodal volcanic-associated massive sulfide systems: Reviews in Economic Geology, v. 8, p. 101–131.

Barrett, T.J., Cattalani, S., and MacLean, W.H., 1991, Massive sulfide deposits of the Noranda area, Quebec: I. The Horne mine: Canadian Journal of Earth Sciences, v. 28, p. 465–488.

Barrie, C.T., 1995, Zircon thermometry of high-temperature rhyolites near volcanic-associated massive sulfide deposits, Abitibi subprovince, Canada: Geology, v. 23, p. 169–172.

Barrie, C.T., Cathles, L.M., and Erendi, A., 1999a, Finite element heat and fluid-flow computer simulations of a deep ultramafic sill model for the giant Kidd Creek volcanic-associated massive sulfide deposit, Abitibi subprovince, Canada: ECONOMIC GEOLOGY MONOGRAPH 10, p. 529–540.

Barrie, C.T., Cathles, L.M., Erendi, A., Schwaiger, H., and Murray, C., 1999b, Heat and fluid flow in volcanic-associated massive sulfide-forming hydrothermal systems: Reviews in Economic Geology, v. 8, p. 201–219.

Bea, F., 1996a, Controls on the trace element composition of crustal melts: Transactions of the Royal Society of Edinburgh, Earth Sciences, v. 87, p. 33–41.

——1996b, Residence of REE, Y, Th, and U in granites and crustal protoliths: Implications for the chemistry of crustal melts: Journal of Petrology, v. 37, p. 521–552.

Bedard, J.H., 2006, A catalytic delamination-driven model for coupled genesis of Archaean crust and sub-continental lithospheric mantle: Geochimica et Cosmochimica Acta, v. 70, p. 1188–1214.

Borisova, A.Y., Pichavant, M., Polve, M., Wiedenbeck, M., Freydier, R., and Candaudap, F., 2006, Trace element geochemistry of the 1991 Mt. Pinatubo silicic melts, Philippines: Implications for ore-forming potential of adakitic magmatism: Geochimica et Cosmochimica Acta, v. 70, p. 3702–3716.

Brauhart, C.W., Groves, D.I., and Morant, P., 1998, Regional alteration systems associated with volcanogenic massive sulfide mineralization at Panorama, Pilbara, Western Australia: ECONOMIC GEOLOGY, v. 93, p. 292–302.

Burnham, O.M., and Schweyer, J., 2004, 54.Trace element analysis of geological samples by inductively coupled plasma mass spectrometry at the Geoscience Laboratories: Revised capabilities due to improvements to instrumentation: Summary of Fieldwork and Other Activities 2004, Ontario Geological Survey Open File 6145, p. 54.1–54.20.

Burnham, O.M., Hechler, J., Semenyna, L., and Schweyer, J., 2002, Mineralogical controls on the determination of trace elements following mixed-acid dissolution: Sudbury, ON, Ontario Geological Survey, p. 36.1–12.

Campbell, I.H., Franklin, J.M., Gorton, M.P., Hart, T.R., and Scott, S.D., 1981, The role of subvolcanic sills in the generation of massive sulfide deposits: ECONOMIC GEOLOGY, v. 76, p. 2248–2253.

Card, K.D., and Poulsen, K.H., 1998, Archean and Paleoproterozoic geology and metallogeny of the southern Canadian Shield: Exploration and Mining Geology, v. 7, p. 181–215.

Cathles, L.M., 1981, Fluid flow and genesis of hydrothermal ore deposits: ECONOMIC GEOLOGY 75TH ANNIVERSARY VOLUME, p. 1905–1980.

——1993, Oxygen isotope alteration in the Noranda mining district, Abitibi greenstone belt, Quebec: ECONOMIC GEOLOGY, v. 88, p. 1483–1511.

Chaloux, E.C., 2005, The Croxall breccia pipe: Geological and geochemical study of an Archean porphyry Cu-Mo-Au system: Unpublished Applied M.Sc. thesis, ON, Laurentian University, 71 p.

Chappell, B.W., White, A.J.R., Williams, I.S., Wyborn, D., and Wyborn, L.A.I., 2000, Lachlan fold belt granites revisited: High- and low-temperature granites and their implications: Australian Journal of Earth Sciences, v. 47, p. 123–138.

Chown, E.H., Harrap, R., and Moukhsil, A., 2002, The role of granitic intrusions in the evolution of the Abitibi belt, Canada: Precambrian Research, v. 115, p. 291–310.

Clemens, J.D., Holloway, J.R., and White, A.J.R., 1986, Origin of A-type granite: Experimental constraints: American Mineralogist, v. 71, p. 317–324.

Corfu, F., 1993, The evolution of the southern Abitibi greenstone belt in light of precise U-Pb geochronology: ECONOMIC GEOLOGY, v. 88, p. 1323–1340.

Corfu, F., and Noble, S.R., 1992, Genesis of the southern Abitibi greenstone belt, Superior province, Canada: Evidence from zircon Hf isotope analyses using a single filament technique: Geochimica et Cosmochimica Acta, v. 56, p. 2081–2097.

Corfu, F., Krogh, T.E., Kwok, Y.Y., and Jensen, L.S., 1989, U-Pb zircon geochronology in the southwestern Abitibi greenstone belt, Superior province: Canadian Journal of Earth Sciences, v. 26, p. 1747–1763.

Cousens, B., Facey, K., and Falck, H., 2002, Geochemistry of the Late Archean Banting Group, Yellowknife greenstone belt, Slave province, Canada: Simultaneous melting of the upper mantle and juvenile mafic crust: Canadian Journal of Earth Sciences, v. 39, p. 1635–1656.

Date, J., Watanabe, Y., and Saeki, Y., 1983, Zonal alteration around the Fukazawa Kuroko deposits, Akita Prefecture, northern Japan: ECONOMIC GEOLOGY MONOGRAPH 5, p. 365–386.

Davis, D.W., 1982, Optimum linear regression and error estimation applied to U-Pb data: Canadian Journal of Earth Sciences, v. 19, p. 2141–2149.

Dimroth, E., Imreh, L., Rocheleau, M., and Goulet, N., 1982, Evolution of the south-central part of the Archean Abitibi belt, Quebec: Part I. Stratigraphy and paleogeographic model: Canadian Journal of Earth Sciences, v. 19, p. 1729–1758.

Drummond, M.S., and Defant, M.J., 1990, A model for trondhjemite-tonalite-dacite genesis and crustal growth via slab melting: Archean to modern comparisons: Journal of Geophysical Research, v. 95, p. B21,503–B21,521.

Drummond, M.S., Defant, M.J., and Kepezhinskas, P.K., 1996, Petrogenesis of slab-derived trondhjemite-tonalite-dacite/adakite magmas: Geological Society of America Special Paper 315, p. 205–215.

Dubé, B., Mercier-Langevin, P., Hannington, M., Lafrance, B., Gosselin, G., and Gosselin, P., 2007, The LaRonde Penna world-class Au-rich volcanogenic massive sulfide deposit, Abitibi, Quebec: Mineralogy and geochemistry of alteration and implications for genesis and exploration: ECONOMIC GEOLOGY, v. 102, p. 633–666.

Feng, R., and Kerrich, R., 1992, Geochemical evolution of granitoids from the Archean Abitibi southern volcanic zone and the Pontiac subprovince, Superior province, Canada: Implications for tectonic history and source regions: Chemical Geology, v. 98, p. 1–2.

Fisher, R.V., 1966, Rocks composed of volcanic fragments and their classification: Earth Science Reviews, v. 1, p. 287–298.

Fowler, A.D., and Jensen, L.S., 1989, Quantitative trace-element modelling of the crystallization history of the Kinojévis and Blake River Groups, Abitibi greenstone belt, Ontario: Canadian Journal of Earth Sciences, v. 26, p. 1356–1367.

Franklin, J.M., Gibson, H.L., Galley, A.G., and Jonasson, I.R., 2005, Volcanogenic massive sulfide deposits: ECONOMIC GEOLOGY 100TH ANNIVERSARY VOLUME, p. 523–560.

Frarey, M.J., and Krogh, T.E., 1986, U-Pb zircon ages of late internal plutons of the Abitibi and eastern Wawa subprovinces, Ontario and Quebec: Geological Survey of Canada Current Research Part A, 86–1A, p. 43–48.

Galley, A.G., 1993, Characteristics of semi-conformable alteration zones associated with volcanogenic massive sulphide districts: Journal of Geochemical Exploration, v. 48, p. 175–200.

——1996, Geochemical characteristics of subvolcanic intrusions associated with Precambrian massive sulphide deposits: Geological Association of Canada Short Course Notes Volume 12, p. 239–278.

——2003, Composite synvolcanic intrusions associated with Precambrian VMS-related hydrothermal systems: Mineralium Deposita, v. 38, p. 443–473.

Galley, A., and van Breemen, O., 2002, Timing of synvolcanic magmatism in relation to base-metal mineralization, Rouyn-Noranda, Abitibi volcanic belt, Quebec: Geological Survey of Canada, 9 p.

Galley, A.G., van Breemen, O., and Franklin, J.M., 2000, The relationship between intrusion-hosted Cu-Mo mineralization and deposits of the Archean Sturgeon Lake mining camp, northwestern Ontario: ECONOMIC GEOLOGY, v. 95, p. 1543–1550.

Galley, A.G., Bailes, A., Hannington, M.D., Holk, G., Katsube, J., Paquette, F., Paradis, S., Santaguida, F., Taylor, B.E., and Hillary, B., 2002, Database for CAMIRO project 94E07: Interrelationships between subvolcanic intrusions, large-scale alteration zones and VMS deposits: Geological Survey of Canada Open-File Report 4431, 9 p.

Galley, A.G., Hannington, M., and Jonasson, I., 2007, Volcanogenic massive sulphide deposits: Mineral Deposits Division, Geological Association of Canada Special Publication 5, p. 141–161.

Gibson, H.L., and Watkinson, D.H., 1990, Volcanogenic massive sulphide deposits of the Noranda cauldron and shield volcano, Québec., in Rive, M., Verpaelst, P., Gagnon, Y., Lulin, J.-M., Riverin, G., and Simard, A., eds., The northwestern Québec polymetallic belt: A summary of 60 years of mining exploration, Rouyn-Noranda: Canadian Institute of Mining and Metallurgy Special Volume 43, p. 119–132.

Gibson, H.L., Kerr, D.J., and Cattalani, S., 2000, The Horne mine: Geology, history, influence on genetic models, and a comparison to the Kidd Creek mine: Exploration and Mining Geology, v. 9, p. 91–111.

Gledhill, T.L., 1928, Ben Nevis, Munro, Kamiskotia, and other base metal areas, Districts of Cochrane and Timiskaming: Ontario Department of Mines, p. 1–52.

Goldie, R., 1978, Magma mixing in the Flavrian pluton, Noranda area, Quebec: Canadian Journal of Earth Sciences, v. 15, p. 132–144.

——1979, Metamorphism of the Flavrian and Powell plutons, Noranda area, Quebec: Journal of Petrology, v. 20, p. 227–238.

Grunsky, E.C., 1986, Recognition of alteration in volcanic rocks using statistical analysis of lithogeochemical data: Journal of Geochemical Exploration, v. 25, p. 1–2.

——1988, Multivariate and spatial analysis of lithogeochemical data from metavolcanics with zones of alteration and mineralization in Ben Nevis Township, Ontario: Unpublished Ph.D. thesis, ON, University of Ottawa, 710 p.

Grunsky, E.C., and Agterberg, F.P., 1988, Spatial and multivariate analysis of geochemical data from metavolcanic rocks in the Ben Nevis area, Ontario: Mathematical Geology, v. 20, p. 825–861.

Hannington, M.D., Santaguida, F., Kjarsgaard, I.M., and Cathles, L.M., 2003, Regional-scale hydrothermal alteration in the Central Blake River Group, western Abitibi subprovince, Canada: Implications for VMS prospectivity: Mineralium Deposita, v. 38, p. 393–422.

Heaman, L.M., 1997, Global mafic magmatism at 2 45 Ga: Remnants of an ancient large igneous province?: Geology, v. 25, p. 299–302.

Hogg, W.A., 1964, Arnold and Katrine Townships: Toronto, Ontario Department of Mines, 13 p.

Hughes, C.J., 1973, Spilites, keratophyres, and the igneous spectrum: Geological Magazine, v. 109, p. 513–527.

Ioannou, S.E., Gotze, J., Weiershauser, L., Zubowski, S.M., and Spooner, E.T.C., 2004, Cathodoluminescence characteristics of Archean volcanogenic massive sulfide related quartz: Noranda, Ben Nevis, and Matagami districts, Abitibi subprovince, Canada: Geochemistry, Geophysics, Geosystems, v. 5, p. doi: 10.1029/2003GC000613 (24 pages).

Irvine, T.N., and Baragar, W.R.A., 1971, A guide to the chemical classification of the common volcanic rocks: Canadian Journal of Earth Sciences, v. 8, p. 523–548.

Jensen, L.S., 1975, Geology of Clifford and Ben Nevis Townships, District of Cochrane: Ontario Geological Survey Geoscience Report GR132 (accompanied by Map 2283).

——1985, Stratigraphy and petrogensis of Archean metavolcanic sequences, southwestern Abitibi subprovince, Ontario: Geological Association of Canada Special Paper 28, p. 65–87.

Jensen, L.S., and Langford, F.F., 1985, Geology and petrogenesis of the Archean Abitibi belt in the Kirkland Lake area, Ontario: Ontario Geological Survey Miscellaneous Paper 123, 130 p.

Jolly, W.T., 1980, The development and degradation of Archean lavas, Abitibi area, Canada: Journal of Petrology, v. 21, p. 323–363.

Kay, S.M., and Mpodozis, C., 2001, Central Andean ore deposits linked to evolving shallow subduction systems and thickening crust: GSA Today, v. 11, p. 4–9.

Kerr, D.J., and Gibson, H.L., 1993, A comparison of the Horne volcanogenic massive sulfide deposit and intracauldron deposits of the Mine Sequence, Noranda, Quebec: ECONOMIC GEOLOGY, v. 88, p. 1419–1442.

King, P.L., Chappell, B.W., Allen, C.M., and White, A.J.R., 2001, Are A-type granites the high-temperature felsic granites? Evidence from fractionated granites of the Wangrah Suite: Australian Journal of Earth Sciences, v. 48, p. 501–514.

Knight, C.W., 1920, Ben Nevis gold area: Ontario Department of Mines, p. 1–27.

Krogh, T.E., 1982, Improved accuracy of U-Pb zircon ages by the creation for more concordant systems using an air abrasion technique: Geochimica et Cosmochimica Acta, v. 46, p. 637–649.

Laflèche, M.R., Dupuy, C., and Bougault, H., 1992a, Geochemistry and petrogenesis of Archean mafic volcanic rocks of the southern Abitibi belt, Quebec: Precambrian Research, v. 57, p. 3–4.

Laflèche, M.R., Dupuy, C., and Dostal, J., 1992b, Tholeiitic volcanic rocks of the Late Archean Blake River Group, southern Abitibi greenstone belt: Origin and geodynamic implications: Canadian Journal of Earth Sciences, v. 29, p. 1448–1458.

Lafrance, B., Davis, D.W., Goutier, J., Moorhead, J., Pilote, P., Mercier-Langevin, P., Dubé, B., Galley, A.G., and Mueller, W.U., 2005, Nouvelle datations isotopiques dan la portion québéquoise du Group de Blake River et des unités adjacentes: Ministeres des Resources Naturelles de la faune et des parcs, Gouvrement de Québec Rapport 2005–1, p. 1–15.

Large, R.R., Gemmell, J.B., Paulick, H., and Huston, D.L., 2001, The alteration box plot: A simple approach to understanding the relationships between alteration mineralogy and lithogeochemistry associated with VHMS deposits: ECONOMIC GEOLOGY, v. 96, p. 957–971.

Lentz, D.R., 1998, Petrogenetic evolution of felsic volcanic sequences associated with Phanerozoic volcanic-hosted massive sulfide systems: the role of extensional geodynamics: Ore Geology Reviews, v. 12, p. 289–327.

Lesher, C.M., Goodwin, A.M., Campbell, I.H., and Gorton, M.P., 1986, Trace element geochemistry of ore-associated and barren felsic metavolcanic rocks in the Superior province, Canada: Canadian Journal of Earth Sciences, v. 23, p. 222–237.

Ludden, J.N., and Peloquin, S.A., 1996, A geodynamic model for the evolution of the Abitibi belt: Implications for the origins of volcanic massive sulphide (VMS) deposits: Geological Association of Canada Short Course Notes, v. 12, p. 205–237.

Ludwig, K.E., 2001, Users manual for Isoplot/Ex v. 2.49: A geochronological toolkit for Microsoft Excel: Berkeley Geochronology Center Special Publication 1a.

MacDonald, P.J., and Piercey, S.J., 2003, 36. Discover Abitibi gold subproject 3. Preliminary regional geological assessment of porphyry intrusions spatially associated with gold deposits in the western Abitibi subprovince, Timmins, Ontario: Summary of Field Work and Other Activities 2003, Ontario Geological Survey Open File 6120, p. 36.1–36.7.

MacDonald, P.J., Piercey, S.J., and Hamilton, M.A., 2005, An integrated study of intrusive rocks spatially associated with gold and base metal mineralization in the Abitibi greenstone belt, Timmins area and Clifford Township: Discover Abitibi Initiative: Ontario Geological Survey Open File Report 6160, 190 p.

Martin, H., Smithies, R.H., Rapp, R., Moyen, J.-F., and Champion, D., 2005, An overview of adakite, tonalite-trondhjemite-granodiorite (TTG), and sanukitoid: Relationships and some implications for crustal evolution: Lithos, v. 79, p. 1–24.

Mercier-Langevin, P., Dube, B., Hannington, M.D., Davis, D.W., Lafrance, B., and Gosselin, G., 2007a, The LaRonde Penna Au-rich volcanogenic massive sulfide deposit, Abitibi greenstone belt, Quebec: Part I. Geology and geochronology: ECONOMIC GEOLOGY, v. 102, p. 585–609.

Mercier-Langevin, P., Dube, B., Hannington, M.D., Richer-Lafleche, M., and Gosselin, G., 2007b, The LaRonde Penna Au-rich volcanogenic massive sulfide deposit, Abitibi greenstone belt, Quebec: Part II. Lithogeochemistry and paleotectonic setting: ECONOMIC GEOLOGY, v. 102, p. 611–631.

Mercier-Langevin, P., Dubé, B., Lafrance, B., Hannington, M., Galley, A., Moorhead, J., and Gosselin, P., 2007c, Metallogeny of the Doyon-Bousquet-LaRonde mining camp, Abitibi greenstone belt, Quebec: Mineral Deposits Division, Geological Association of Canada Special Publication 5, p. 673–701.

Miller, C.F., Meschter McDowell, S., and Mapes, R.W., 2003, Hot and cold granites? Implications of zircon saturation temperatures and preservation of inheritance: Geology, v. 31, p. 529–532.

Mortensen, J.K., 1993, U-Pb geochronology of the eastern Abitibi suprovince. Part 2: Noranda-Kirkland Lake area: Canadian Journal of Earth Sciences, v. 30, p. 29–41.

Moyen, J.-F., and Stevens, G., 2006, Experimental constraints on TTG petrogenesis: Implications for Archean geodynamics: Geophysical Monograph 164, p. 149–175.

O'Connor, J.T., 1965, A classification for quartz-rich igneous rocks based on feldspar ratio: U.S. Geological Survey Professional Paper 525B, p. 79–84.

Paradis, S., Ludden, J.N., and Gelinas, L., 1988, Evidence for contrasting compositional spectra in comagmatic intrusive and extrusive rocks of the Late Archean Blake River Group, Abitibi, Quebec: Canadian Journal of Earth Sciences, v. 25, p. 134–144.

Paradis, S., Taylor, B.E., Watkinson, D.H., and Jonasson, I.R., 1993, Oxygen isotope zonation and alteration in the northern Noranda district, Quebec: Evidence for hydrothermal fluid flow: ECONOMIC GEOLOGY, v. 88, p. 1512–1525.

Pearce, J.A., 1996, A user's guide to basalt discrimination diagrams: Geological Association of Canada Short Course Notes, v. 12, p. 79–113.

Péloquin, A.S., 1999, Reappraisal of the Blake River Group stratigraphy and its place in the Archean volcanic record: Unpublished thèse de doctorat thesis, Montreal, QP, Université de Montréal, 189 p.

Péloquin, A.S., and Piercey, S.J., 2003, 41. Discover Abitibi.base metal subproject 3: Geology and base metal mineralization in Ben Nevis, Katrine, and Clifford Townships: Summary of Field Work and Other Activities 2003, Ontario Geological Survey Open File 6120, p. 41.1–41.8.

——2005, Discover Abitibi project, base metal subproject 3: Geology and base metal mineralization in Ben Nevis, Katrine and Clifford Townships: Sudbury, ON, Ontario Geological Survey Open File Report 6161, 86 p.

Péloquin, S.A., Potvin, R., Paradis, S., Laflèche, M.R., Verpaelst, P., and Gibson, H.L., 1990, The Blake River Group, Rouyn-Noranda area, Quebec: A stratigraphic synthesis: Canadian Institute of Mining and Metallurgy Special Volume 43, p. 107–118.

Péloquin, A.S., Piercey, S.J., and Hamilton, M.A., 2008, The Ben Nevis Volcanic Complex, Ontario, Canada: Part of the late volcanic phase of the Blake River Group, Abitibi subprovince: ECONOMIC GEOLOGY, v. 103, p. 1219–1241.

Piercey, S.J., Hamilton, M.A., Peloquin, A.S., and Chaloux, E., 2004, 44.Discover Abitibi project, intrusion subproject: Updates on studies of the Clifford stock and Blake River Group, Clifford Township: Summary of Fieldwork and Other Activities 2004, Ontario Geological Survey Open File 6145, p. 44.1–44.14.

Piercey, S.J., Mortensen, J.K., and Creaser, R.A., 2003, Neodymium isotope geochemistry of felsic volcanic and intrusive rocks from the Yukon-Tanana terrane in the Finlayson Lake region, Yukon, Canada: Canadian Journal of Earth Sciences, v. 40, p. 77–97.

Powell, W.G., Carmichael, D.M., and Hodgson, C.J., 1993, Thermobarometry in a subgreenschist to greenschist transition in metabasites of the Abitibi greenstone belt, Superior province, Canada: Journal of Metamorphic Geology, v. 11, p. 165–178.

——1995, Conditions and timing of metamorphism in the southern Abitibi greenstone belt, Quebec: Canadian Journal of Earth Sciences, v. 32, p. 787–805.

Racicot, D., 1990, La production minière dans la partie Québécoise de la Sous-province d'Abitibi: 1927–1988: Canadian Institute of Mining and Metallurgy Special Volume 43, p. 33–42.

Rapp, R.P., and Watson, E.B., 1995, Dehydration melting of metabasalt at 8–32 kbar: Implications for continental growth and crust-mantle recycling: Journal of Petrology, v. 36, p. 891–931.

Rapp, R.P., Watson, E.B., and Miller, C.F., 1991, Partial melting of amphibolite/eclogite and the origin of Archean trondhjemites and tonalites: Precambrian Research, v. 51, p. 1–25.

Richards, J.P., 2003, Tectono-magmatic precursors for porphyry Cu-(Mo-Au) deposit formation: ECONOMIC GEOLOGY, v. 98, p. 1515–1534.

Richards, J.P., and Kerrich, R., 2007, Adakite-like rocks: Their Diverse Origins and Questionable Role in Metallogenesis: ECONOMIC GEOLOGY, v. 102, p. 537–576.

Riopel, J., Hubert, C., Cattalani, S., Barrett, T.J., and Hoy, L.D., 1995, Gîtologie, structure et géochimie du gisement de sulfures massifs Mobrun, (district de Rouyn-Noranda): Ministère de Ressources naturelles du Québec Rapport ET 92–02, 142 p.

Saeki, Y., and Date, J., 1980, Computer application to the alteration data of the footwall dacite lava at the Ezuri Kuroko deposits, Akito Prefecture: Mining Geology, v. 30, p. 241–250.

Selby, D., and Creaser, R.A., 2001a, Late and Mid-Cretaceous mineralization in the northern Canadian Cordillera: Constraints from Re-Os molybdenite dates: ECONOMIC GEOLOGY, v. 96, p. 1461–1467.

——2001b, Re-Os geochronology and systematics in molybdenite from the Endako porphyry molybdenum deposit, British Columbia, Canada: ECONOMIC GEOLOGY, v. 96, p. 197–204.

——2004, Macroscale NTIMS and microscale LA-MC-ICP-MS Re-Os isotopic analysis of molybdenite: Testing spatial restrictions for reliable Re-Os age determinations, and implications for the decoupling of Re and Os within molybdenite: Geochimica et Cosmochimica Acta, v. 68, p. 3897–3908.

Skjerlie, K.P., and Johnston, A.D., 1992, Vapor-absent melting at 10 kbar of a biotite- and amphibole-bearing tonalitic gneiss: Implications for the generation of A-type granites: Geology, v. 20, p. 263–266.

Spitz, G., and Darling, R., 1978, Major and minor element lithogeochemical anomalies surrounding the Louvem copper deposit, Val d'Or, Quebec: Canadian Journal of Earth Sciences, v. 15, p. 1161–1169.

Stacey, J.S., and Kramer, J.D., 1975, Approximation of terrestial lead isotope evolution by a two-stage model: Earth and Planetary Science Letters, v. 26, p. 207–221.

Steiger, R.H., and Jäger, E., 1977, Subcommision on geochronology: Convention in the use of decay constants in geo- and cosmochronology: Earth and Planetary Science Letters, v. 36, p. 359–362.

Sutcliffe, R.H., Barrie, C.T., Burrows, D.R., and Beakhouse, G.P., 1993, Plutonism in the southern Abitibi subprovince: A tectonic and petrogenetic framework: ECONOMIC GEOLOGY, v. 88, p. 1359–1375.

Taylor, B.E., Holk, G.J., and Huston, D.L., 2000, Oxygen isotope mapping and evaluation of palaeo-hydrothermal systems associated with synvolcanic intrusions and VMS deposits: Centre for Ore Deposit and Exploration Studies (CODES), Hobart, University of Tasmania, Special Publication. 3, p. 207–208.

Thurston, P.C., Ayer, J.A., Goutier, J., and Hamilton, M.A., 2008, Depositional gaps in Abitibi greenstone belt stratigraphy: A key to exploration for syngenetic mineralization: ECONOMIC GEOLOGY, v. 103, p. 1097–1134.

Watkins, J.J., and Melling, D.R., 2004, Progress report on mineral exploration, Verna Lake area, Ben Nevis property: Sudbury, ON, Wallbridge Mining Company Ltd., 82 p.

Watson, E.B., 1996, Dissolution, growth and survival of zircons during crustal fusion: Kinetic principles, geological models and implications for isotopic inheritance: Transactions of the Royal Society of Edinburgh, Earth Sciences., v. 87, p. 43–56.

Watson, E.B., and Harrison, T.M., 1983, Zircon saturation revisited: Temperature and composition effects in a variety of crustal magma types: Earth and Planetary Science Letters, v. 64, p. 295–304.

Weiershauser, L., and Spooner, E.T.C., 2005, Seafloor hydrothermal fluids, Ben Nevis area, Abitibi greenstone belt: Implications for Archean (~2.7 Ga) seawater properties: Precambrian Research, v. 138, p. 89–123.

Whalen, J.B., McNicoll, V.J., Galley, A.G., Longstaffe, F.J., and Percival, J.A., 2004, Tectonic and metallogenic importance of an Archean composite high- and low-Al tonalite suite, western Superior province, Canada: Precambrian Research, v. 132, p. 275–301.

Wilson, W.J., 1901, Western part of the Abitibi region: Geological Survey of Canada, Summary Report, Part A, p. 117A-130A.

Winchester, J.A., and Floyd, P.A., 1977, Geochemical discrimination of different magma series and their differentiation products using immobile elements: Chemical Geology, v. 20, p. 325–343.

Wolf, M.B., and Wyllie, P.J., 1994, Dehydration-melting of amphibolite at 10 kbar: the effects of temperature and time: Contributions to Mineralogy and Petrology, v. 115, p. 369–383.

Wolfe, W.J., 1977, Geochemical exploration of Early Precambrian volcanogenic massive sulphide mineralization in Ben Nevis Township, District of Cochrane: Ontario Geological Survey Study 19, 39 p.

Wyllie, P.J., Wolf, M.B., and van der Laan, S.R., 1997, Conditions for formation of tonalites and trondhjemites: Magmatic sources and products: Oxford Monographs on Geology and Geophysics 35, p. 256–266.

Wyman, D.A., 2003, Upper mantle processes beneath the 2 7 Ga Abitibi belt, Canada: A trace element perspective: Precambrian Research, v. 127, p. 1–3.

Wyman, D.A., Kerrich, R., and Polat, A., 2002, Assembly of Archean cratonic mantle lithosphere and crust: Plume-arc interaction in the Abitibi-Wawa subduction-accretion complex: Precambrian Research, v. 115, p. 37–62.